ADDIS ABABA UNIVERSITY

ADDIS ABABA INSTITUTE OF TECHNOLOGY

SCHOOL OF CHEMICAL AND BIOENGINEERING

ENVIRONMENTAL ENGINEERING

REMOVAL OF LEAD FROM WASTEWATER USING MODIFIED KAOLIN (ZEOLITE-X)

BY:

ALEMSHET GHION MELAKU

JULY, 2023

ADDIS ABABA

REMOVAL OF LEAD FROM WASTEWATER USING MODIFIED KAOLIN (ZEOLITE-X)

BY:

ALEMSHET GHION MELAKU

A THESIS SUBMITTED TO ADDIS ABABA UNIVERSITY INSTITUTE OF TECHNOLOGY SCHOOL OF CHEMICAL AND BIOENGINEERING IN PARTIAL FULFILLMENT OF THE REQUIREMENT FOR THE MASTER'S DEGREE IN ENVIRONMENTAL ENGINEERING

ADVISOR:

PROFESSOR ENG. ZEBENE KIFLIE

JULY, 2023

ADDIS ABABA

APPROVAL SHEET

ADDIS ABABA UNIVERSITY

ADDIS ABABA INSTITUTE OF TECHNOLOGY (AAIT) SCHOOL

OF CHEMICAL AND BIO ENGINEERING

M.Sc. in Environmental Engineering

As members of the Examining Board of the final M.Sc. open defense, we certify that we have read and evaluated the thesis prepared by Alemshet Ghion Entitled: " **Removal of Lead from Wastewater using Modified Kaolin (Zeolite-X)**" That it has been accepted as fulfilling the thesis requirement for the degree of Masters of Science in Environmental engineering.

_____	_____	_____
Name of advisor	Signature	Date
_____	_____	_____
Name of Chairman	Signature	Date
_____	_____	_____
Name of External Examiner	Signature	Date
_____	_____	_____
Name of Internal Examiner	Signature	Date

DECLARATION

I declare that this thesis entitled Removal of Lead from Wastewater using Modified Kaolin (Zeolite-X) is my own original work done under the supervision of Prof. Eng. Zebene Kiflie at School of Chemical and Bio engineering in Addis Ababa Institute of Technology, Addis Ababa University and I have not previously submitted it entirely or in part for obtaining any qualification at any other university

Name: Alemeshet Ghion Melaku

Signature: _____

Date of submission _____

ACKNOWLEDGEMENTS

First of all, I would like to thank God for giving me the courage and strength to go through the entire course as well as this research.

I wish to express my deepest and sincere gratitude to my advisor Professor Eng. Zebene Kiflie whose encouragement, guidance, and support both technical and academic enabled me to realize this research work. I also wish to express my deepest gratitude for your dedicated advice, closer help, and warmest treatments besides the ideas, suggestions, and title for this current work. Thank you, Professor, for teaching me not only academic matters but also how to use proper properties and budgeting time.

It is also my pleasure to express my gratitude to the management of Nefas Silk Paint Factory for all the support given to me during my studies. I would also extend my thanks to the Addis Ababa University chemistry department for the study, the employees involved in responding to characterization and analysis results, and those colleagues who worked together with me in the data collection. I am so indebted to those who generally assisted me directly or indirectly in providing their suggestions, support, and data collection.

Finally, the moral support given by Hintsa Selassie Seifu, Solomon Wondimu, Miherete Demelash, my mother, and my sister Ababa Ghion was a source of strength and determination in my studies. Their sacrifice, patience, understanding, warmth, and love have made this research study a meaningful endeavor. My thanks are also extended to my family in general but special respect goes to my brother Dagnachew Ghion since his contribution to the completion of this thesis was so immense.

Finally, I am very thankful to Addis Ababa University Institute of Technology without its resources my work would have not been realized.

TABLE OF CONTENTS

LIST OF FIGURES

Page

LIST OF TABLES

LIST OF SYMBOLS AND ACRONYMS

AAS	Atomic Absorption Spectroscopy
b	Langmuir constant (L/mg)
CEC	Cation Exchange Capacity
^0C	Degree centigrade
C_0	Initial Lead (II) ion ions concentration in a liquid phase (mg/L)
Ce	Lead (II) ion ion concentration after adsorption in a liquid phase at equilibrium (mg/L)
FTIR	Fourier Transfer Infrared Spectroscopy
FAU	Faujasite
IUPAC	International Union of Pure and Applied Chemistry
K_1	First order rate constant (min^{-1})
K_2	Second order rate constant (g/mg min)
K_F	Freundlich capacity factor (mg/g)
1/n	Freundlich intensity parameter
M	Weight of the adsorbent (g)
Na-X	Zeolite-X
PBU	Primary building unit
pH	Power of Hydrogen
ppm	parts per million (10^{-6})
q_e	Adsorption capacity at equilibrium (mg/g)
q_{max}	Maximum adsorption capacity (mg/g)
q_t	Adsorption capacity at time t (mg/g)
rpm	Revolutions per minute
R_L	Separation factor
SBU	Secondary building unit
SEM	Scanning Electron Microscopy
WHO	World Health Organization
XRD	X-Ray Diffraction
VIF	Variance Inflation Factor

ABSTRACT

the objective of this study was to investigate the lead (II) ion removal efficiency of modified kaolin (zeolite X) from wastewater. By using batch experiments, zeolite-X was synthesized, characterized, and applied to adsorb lead from wastewater. In this study, the synthesis of zeolite-X was performed at 600 0C for 1 h in a muffle furnace from kaolin formed as meta-kaolin and then mixed with NaOH. The adsorbent was characterized using XRD, FTIR, SEM, and BET. The concentration of the lead ion was determined using atomic absorption spectrophotometer (AA 2400FS Varian. The XRD revealed that zeolite-X synthesized has a faujasite (FAU) phase, composed of cubic, rectangular, and irregular crystallite shapes as seen by SEM. The FTIR analysis revealed the presence of functional groups Si-O bonds associated with zeolite. The BET analysis show that the adsorbent is porous and has good surface area to adsorb lead. The effects different factors on the Lead (II) ion removal efficiency was studied in batch adsorption experiments. Results show that Lead (II) ion the removal efficiency of the prepared adsorbent was dependent on the pH, contact time, adsorbent dosage and Lead (II) ion initial concentration. Experiment results showed that maximum removal of lead (II) ion by zeolite-X at optimum condition (5.2 pH, 51.8min contact time, 4.506 g adsorbent dose and 12.8mg/L initial concentration of lead(II)ion) is 98.2 %..Adsorption data were interpreted in terms of Langmuir and Freundlich isotherms. It was observed that the experimental data fitted better to Langmuir model with a correlation factor (R^2) value of 0.99996 compared to Freundlich with R^2 value of 0.85075and the maximum adsorption capacity of the material was 39.67 mg of Pb/g of zeolite-X. The kinetic processes of Lead (II) ion adsorption on zeolite -X were described by applying pseudo-first-order and pseudo-second-order kinetic models. The kinetic data for the adsorption process obeyed a pseudo-second-order kinetic model with regression coefficients value of 0.999561, suggesting that the adsorption process is chemisorption. The synthesized zeolite -X showed good potential for the removal of Lead (II) ion from aqueous solution and it also removes lead (II) ion from the real Nefas silk paint industry waste water about 90.9%.

***Key words**: Kaolin, Zeolite-X, Adsorption, Lead (II) ion, wastewater*

1. INTRODUCTION

1.1. Background of the Study

Water is a limited natural resource that is essential for survival and well-being. Saltwater accounts for approximately 97.5% of all water on Earth, with fresh water accounting for the remaining 2.5%. The Antarctic and Greenland ice caps contain around 70% of the world's fresh water. Only 1% of the world's purified is available for extraction and human use. Water is essential for life as well as the processing of numerous materials in the industry. Living species cannot survive without water, and nearly all businesses rely on it to function. However, in the twenty-first century, the rising population and industrial sector have considerably contributed to a loss in water quality and availability through the discharge of untreated wastewater into the environment, which has become a worry for many nations across the world (Tesfaye, 2016).

Environmental pollution is a major challenge facing many developing countries in this present time. Environmental pollution of water bodies has become a great concern and threat to aquatic life as well as humans. Rapid industrialization and urbanization have led to the generation of toxic heavy metals which pollute the environment (Afolabi, et al, 2021).

The discharge of wastes into the water bodies by man had brought about modification of the environmental water quality, hence making substantial quantities of water unsuitable for various uses. Compromise in the quality of the environment as a result of effluent discharge from the industrial sectors has become an environmental issue for many countries especially developing nations like Ethiopia (Aniyikaiye et al. 2019)

It is reported that around 70% of the industrial wastes in developing nations are disposed of untreated into waters thereby contaminating the existing water supplies (Shrestha, Neupane, and Bisht, 2017). A number of studies have indicated that among industries located in Ethiopia, 90 to 96 percent discharge their waste without any form of treatment to nearby water bodies and open spaces (Tadesse et al, 2018). The disposal of untreated wastewater from various industries, urban wastes, and agrochemical wastes in low land, open water bodies has reached an alarming situation in Ethiopia which is increasing day by day (Menbere, 2019).

Uncontrolled urbanization and inadequate sanitary facilities in Ethiopia are causing substantial-quality degradation of surface waters as a result of the country's growing population. Water contamination from the dumping of industrial wastewater is becoming a major concern in Addis Ababa and the surrounding areas, where the majority (more than 40%) of large and medium-scale manufacturing businesses are located. As a result, many rivers and streams that pass through major cities and towns are extremely polluted. Point sources, such as single-source industrial discharges and wastewater treatment plants, can pollute surface waters. The majority of contaminants, in addition, come from non-point sources (Hamere Yohannes and Eyasu Elias 2017).

Widespread use of lead in various industries such as battery manufacturing, radiation shielding, acid metal plating, ammunition, tetraethyl lead manufacturing, ceramic and glass industries printing, painting , water piping, laundry processes, textile radiator manufacturing, pigment and paint production, mining operations, and glass, and other industries can release lead into environment (Chai et al. 2020; Safatian et al. 2019) .

Recent research designed to measure lead (II) ion contamination level in drinking water in Addis Ababa and assess the associated health risks has shown that the mean concentration of lead (II) ion was 17.8 μg/l, where more than 50% of the samples exceeded WHO's 10 μg/L guideline(Endale et al. 2021). Heavy metal content and physico chemical properties of effluent samples collected from different paint industries were studied by Woldeamanuale (2017). The study reported that the maximum concentration of lead (II) ion was 53.4mg/L in effluent samples collected from rainbow paint manufacturing industry, while second largest contribution of 24.84 mg/L was found in the effluents of Zemillic paint manufacturing industry.

Table 1.1: Lead content and Physico Chemical properties of Effluent Samples Collected from different paint industries

Parameter	Name of paint industries				
	Nifas Silk	**Zemillic**	**Cadisco**	**Bright**	**Rainbow**
pH	6.72	7.16	6.77	6.48	7.7
SS	6912.5	9525	1965	8862.5	32528
PO-24	15.37	41.8	2.265	44.5	65.375
BOD	350	246	47	360	600
COD	1949	3524	425	288.7	7662.5
Cr	9.32	8.25	1.5	5.28	2.95
Pb	8.33	24.84	0.68	18.73	53.4
Cd	7.813	2.47	1.58	16.82	69.22
Cu	2.24	9.22	2.09	189.16	22.47
Ag	5.69	15.23	6.08	28.06	14.72

All parameters are mg/L except pH(Woldeamanuale 2017) All units are in mg/L except pH.

Several different processes have been developed for the removal of heavy metals from aqueous media such as electrodialysis, chemical precipitation, adsorption, solvent extraction, reverse osmosis, ultrafiltration, or ion exchange. The adsorption process has shown good effectiveness, efficiency, and economic feasibility in removing heavy metals such as lead from aquatic samples (Safatian et al. 2019). The key benefits of the adsorption method for heavy metal removal are lower operational costs, unproblematic design, and easy operation (Nur-E-Alam et al. 2020).

An efficient adsorbent for extracting Pb (II) ions from water solutions and paint production effluent, according to a recent study, is activated carbon made from the stems of the Canna indica plant. With an initial Pb (II) ion concentration of 102.4 mg/L, a dosage of 1.4 g of

adsorbent, and a pH of 5.5, better removal (98%) was achieved compared to 69.7% of Pb (II) ions removed from the paint industry effluent under the same circumstances(Tessema, Adugna, and Kamaraj 2020). The efficiency of activated carbon in removing Pb (II) ions was significatly lower than in water solutions because paint effluent from manufacturers contains numerous pollutants (Tessema et al., 2020). However, natural kaolin, which is cheap and plentiful, is more costly and less selective than activated carbon. Because of its porosity, and uniform pure crystallite.

Zeolites are hydrated aluminum silicates of alkaline earth or alkali metals that are crystalline and micro-porous(Ibrahim et al. 2022). The frameworks are made of $[SiO_4]^{4-}$ and $[AlO_4]^{5-}$tetrahedral elements that corner-share to generate various open configurations. The positive charge of ions positioned at specified places of the zeolite framework compensates for the negative charge of the lattice. The compensating cations in most zeolites are generally monovalent and bivalent metal ions and their combinations. (Gougazeh and colleagues, 2018)

Synthetic zeolites with a faujasite structure (FAU) have been shown to be effective at removing Pb(II) ion from wastewater (Medina-Rodríguez et al. 2021). In light of the above, this research aims to synthesize zeolite from Ethiopian clay and evaluate its potential as an adsorbent for the removal of Pb(II) ion. The influences of important parameters such as lead metal ion concentration in aqueous solution, contact time, adsorbent dosage, and pH was investigated.

1.2. Statement of the Problem

Heavy metals are poisonous, persist in the environment, pollute food chains, and result in a variety of health issues. Chemicals that have been discharged into the water can affect hormones and cause cancer. The discharge of industrial wastewater is also unquestionably recognized to have a bright color, a pH that fluctuates greatly, a high temperature, a high COD and BOD content, and a significant number of suspended particulates. Extreme industrial effluent pollution endangers the health of nearby residents, reduces soil fertility, and kills fish and aquatic life. A thorough audit and characterization of wastewater produced by industrial operations serve as the first step in the avoidance of pollution of water (Abu Bakar et al., 2020).

Lead contamination is a severe environmental hazard, and even at low levels, lead is a harmful inorganic pollutant in surface and groundwater (Mekuria, Kassegne, and Asfaw, 2020; Odaracha et al., 2021). The presence of even tiny amounts of Pb (II) ion in environmental samples causes pollution and a variety of fatal disorders, including kidney damage and neurological system failure. Pb (II) ion accumulates quickly in the blood, kidney, reproductive system, neurological system, and brain, and acute lead poisoning can cause colic shock, severe anemia, and permanent damage to the brain Lead poisoning affects the central nervous system, and is specifically harmful to children (Fu and Wang, 2011). The toxicity of Pb (II) ion has been identified in natural water systems all over the world, and WHO established 0.05 mg/L of Pb (II) ion as the level allowed.

In Ethiopia, most paint factories do not properly treat the wastewater but rather discharge it directly to the river. So far, many processes for the removal of toxic pollutants from water and wastewater have been proposed. Chemical precipitation, and physical treatment such as electrochemical reduction, ion exchange, and membrane separation are some of the processes that have been reported to be the most effective ones in the removal of heavy toxic pollutants. However, these processes involve the use of chemicals and synthetic polymers which damage the environment.

Nefas Silk Lafto, a sub-city of Addis Abeba, Ethiopia, is home to the Nefas Silk paint facility. The earliest paint industry in Ethiopia is the Nefas Silk Paints Industry. Since 1967, the firm has been manufacturing paints for wood, metal, and wall as well as varnishes, antirust, board paints,

automotive paints, glues, traffic and road markings, industrial paints, and other products. According to data from the Nefas Silk Paints facility from 2005 to 2010, the facility can create a maximum of 87,671 liters of paint per day and as a result, produces an average of two thousand liters of liquid waste daily. Since its creation, untreated sewage has been leaking into the Akaki River. The waters of the river keep flowing to the Aba Samuel Stream's main channel. According to Malakootian et al. (2009), paint wastewater is one of the more difficult, bothersome, and potent industrial waste products due to its high chemical oxygen demand (COD), total suspended solids (TSS), and heavy metal content (Irshad et al. 2023). The paint effluent frequently contained significant levels of COD, total suspended solids (TSS), and heavy metals, with corresponding ranges of 0.1 to 15.5 mg/L, 6,000 to 6,500 mg/L, and 3,000 to 3,500 mg/L (Sime, 2018).

Pb transferred a proportionally higher amount from soil to grass and from grass to milk than Cd. Therefore, Lead is selected for this study as Table 1 shows from a recent study of high effluent from paint, especially Nefas silk paint factory. Taking this into account this study was concerned with the evaluation of the removals of lead from Nefas Silk paint factory wastewater using synthetic zeolite -X prepared from natural Kaolin.

1.3. Objectives of the Study

1.3.1. General Objective

The objective of this study was to investigate the lead (II) ion removal efficiency using modified kaolin (zeolite-X) from paint factory wastewater.

1.3.2. Specific Objectives

The specific objectives of this study are:

- ✓ To use and apply the cheap source Ethiopian kaolin for the preparation of zeolite X.
- ✓ To Confirm and assure the formation and the structure of zeolite X using characterization techniques x-ray diffraction (XRD), FTIR, A Brunauer- Emmett-Teller (BET) and scanning Electron microscopy (SEM).
- ✓ To investigate the effect of operating parameters such as pH, contact time, adsorbent dosage, and Lead (II) ion concentration on the removal efficiency of modified kaolin (zeolite x).
- ✓ To improve and enhance the Lead(II) ion removal conditions from waste water

1.4. Significance of the Study

Scientists in the world search for newer and cheaper choices to treat wastewater. Adsorption is one such method that has gained popularity in recent years. This work investigated the removal of lead ions from lead-contaminated water using zeolite–X. In addition, it substitutes zeolites imported for the purification of water at a high cost. When Activated carbon is compared to the synthesis, cost of zeolite preparation is low. It is also environmentally friendly since no carbon emissions.

1.5. Scope of the Study

This study focuses on the removal of lead (II) ion from wastewater based on the preparation of zeolite-X from Ethiopian kaolin in the laboratory of Addis Ababa University and Nefas Silk paint factory.

2. LITERATURE REVIEW

2.1. Historical Background of Zeolite

Zeolites are a family of crystalline aluminosilicate minerals. The history of zeolites began in 1756 when the Swedish mineralogist Cronstedt discovered the first zeolite mineral. Zeolite is from two Greek words zein and lithos meaning “boiling" and “stone” respectively. Since then, zeolite has been recognized as a separate group of minerals, one of the most abundant on Earth. Zeolites are microporous crystalline materials with stable structures consisting of molecular-sized pores and channels. The structure of zeolites contains aluminum, silicon, and oxygen in regular frameworks with cation and water in the porous (Bavel et al. 2020).

Zeolites come in two varieties: natural zeolites and artificial zeolites. There are over fifty recognized natural zeolites. Each of them is unique in terms of chemical makeup and structure.Analcime, chabazite, clinoptilolite, heulandites, erionite, ferrierite, laumontite, mordenite, and phillipsite are the most prevalent minerals. More than 200 of them have been created by synthetic means for particular uses which are adsorbent materials, cation exchangers, and industrial catalysts. (Bavel et al. 2020)

More than 200 synthetic zeolites have been described and proved to have a more homogeneous composition than natural zeolites. Synthetic zeolites have larger surface areas, and larger micropore volumes, are free of contaminants, and may be tailored to a specific application. For various applications, a significant variety of distinct zeolites with differing functional groups have been synthesized. The most prevalent synthetic zeolites are zeolites A, X, Y, and ZSM-5 (Moshoeshoe et al, 2017).

Zeolites are crystalline inorganic polymers composed of tetrahedral [SiO4] and [AlO4] ions and water molecules with a high degree of freedom of movement. The distinctive features of zeolites are due to their particular structure (Magdalena et al. 2020). The presence of channels and chambers with strictly defined dimensions (shape-selectivity); a high degree of hydration and the presence of so-called "zeolite water"; a high degree of crystallinity; the possibility of sorption of molecules and ions; ion exchange capacity; catalytic properties are among the most significant potential uses. These zeolitic features pique the curiosity of chemists, technologists, and

mineralogists (Magdalena et al. 2020)Zeolites are crystalline, micro porous, hydrated alumino silicates that are built from an infinitely extending three-dimensional network of $[SiO_4]^{4-}$ and $[AlO_4]^{5-}$ tetrahedral linked to each other by the sharing of oxygen atoms. Generally, their structure can be considered as inorganic polymer built from tetrahedral TO_4 units, where T is Si^{4+} or Al^{3+} ion. Each O atom is shared between two T atoms.

The structure formula of zeolite is based on the crystallographic unit cell Mx/n [(AlO2)x(SiO2)y] • wH_2O, where M is an alkali or alkaline earth cation, n is the valence of the cation, w is the number of water molecules per unit cell, x and y are the total number of tetrahedra per unit cell, and the ratio y/x usually has values of 1 to 5, though, for the silica zeolite, y/x can be ranging from 10 to 100. The tetrahedral forms a structural framework in zeolites with centrally located Si or Al atoms and corners occupied by oxygen atoms being shared between SiO_4 and AlO_4, oriented in such a way that the framework develops voids or pores in the form of cages and channels. As an example, zeolite-X also called Na-X [i.e., Na88 (AlO_2)88 (SiO_2)104. 220H_2O, where X is 88, Y is 104 and hence Y/X is 1.2 which is between 1 and 5] (Markovska 2018)

All zeolites are composed of an elementary structure of an aluminosilicate framework which comprises a tetrahedral arrangement of silicon cations (Si^{4+}) and aluminum cation (Al^{3+}) that are surrounded by four oxygen anions (O^{2-}). Each oxygen ion within the Si-O and Al-O bonds connects two cations and is shared between two tetrahedrons (as shown in Figure 2.1), thus yielding a three-dimensional macromolecular framework of SiO^2 and AlO^2 tetrahedral building blocks. In this arrangement of atoms, each tetrahedron consists of four O atoms surrounding a Si or Al cation, resulting in a three-dimensional structure of silicate tetrahedral with a Si: O ratio of 1:2 (Moshoeshoe, et al, 2017).

Some Si4+ ions are substituted by Al^{3+} ions, resulting in a net negative charge in the tectosilicate framework (figures 2.1 and 2.3). This charge arises from the difference in formal valence between the $(AlO_4)^{5-}$ and $(SiO_4)^{4-}$ tetrahedrons and is normally located on one of the oxygen anions connected to an aluminum cation. The resulting negative sites are balanced by counter ions which are usually alkaline or alkaline earth metals, such as Na^+, K^+, or Ca^{2+} in most cases. Li^+, Mg^{2+}, $Sr^{2+,}$ and Ba^{2+} are also found in some zeolites. These ions are found on the external surface of zeolite, bound with the aluminosilicate structure by weaker electrostatic bonds

(Moshoeshoe, etal.,2017).

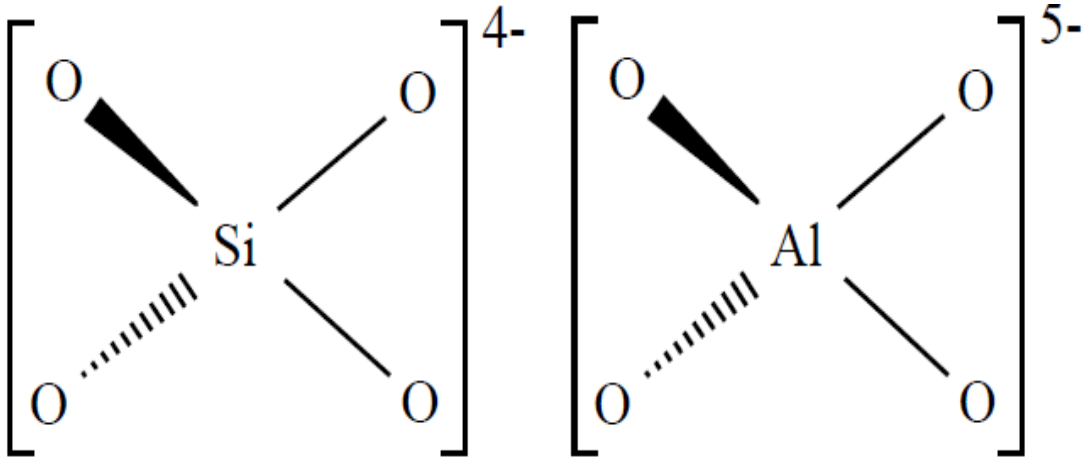

Figure 2.1. The tetrahedral arrangement of the SiO_4 and AlO_4 molecules forming unit blocks of a zeolite (Moshoeshoe,et al , 2017)

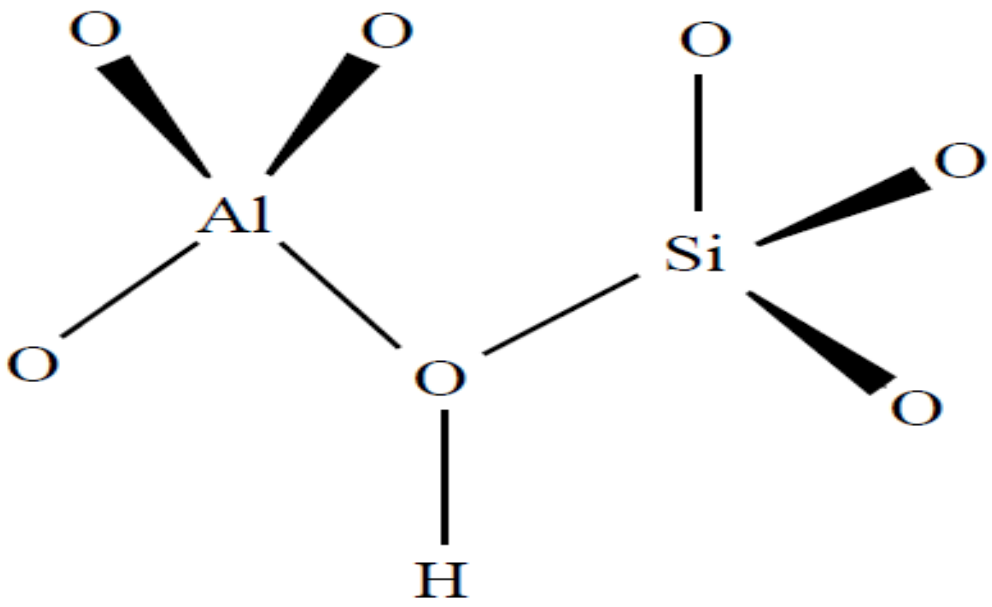

Figure 2.2:Tetrahedral arrangement of the Si-O and Al-O bonds forming a unit block of a zeolite(Moshoeshoe, et al, 2017)

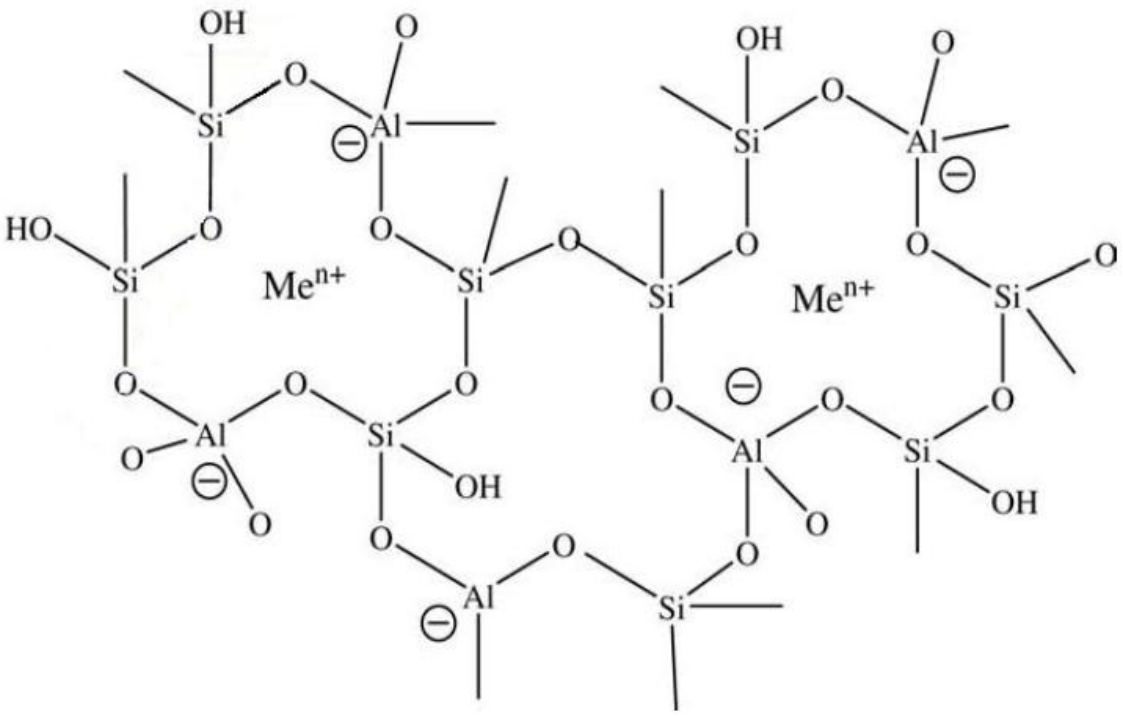

Figure 2.3.A two-dimensional representation of the framework structure of zeolites. Me^{n+} signify extra framework cation (Moshoeshoe, et al. 2017).

2.2. Kaolin

Kaolin is inexpensive, naturally occurring, abundant material and employed as the only source of silica and alumina. The name kaolin comes from the Chinese term "kaoliang" meaning high ridge. In 1867, Johnson and Blake were the first to use the name kaolinite for the mineral of kaolin. Kaolinite is the most important clay mineral of kaolin (figure 2.4), whose chemical formula is Al_2O_3 $2SiO_2.2H_2O$ ($Al_2Si_2O_5$ $(OH)_4$), and its composition expressed in oxides is 46.54% SiO_2, 39.50% Al_2O_3, 13.96% H_2O with a 1:1 uncharged dioctahedral layer structure (Masoudian et al, 2013).

Kaolin as found in nature usually contains varying amounts of other minerals such as muscovite, quartz, feldspar, and anatase. In addition, crude kaolin is frequently stained yellow by iron hydroxide pigments. It is often necessary to bleach the clay chemically to remove the iron pigment and to wash it with water to remove the other minerals in order to prepare kaolin for commercial use.

Figure 2.4.Kaolin plate(Ayele et al. 2015)

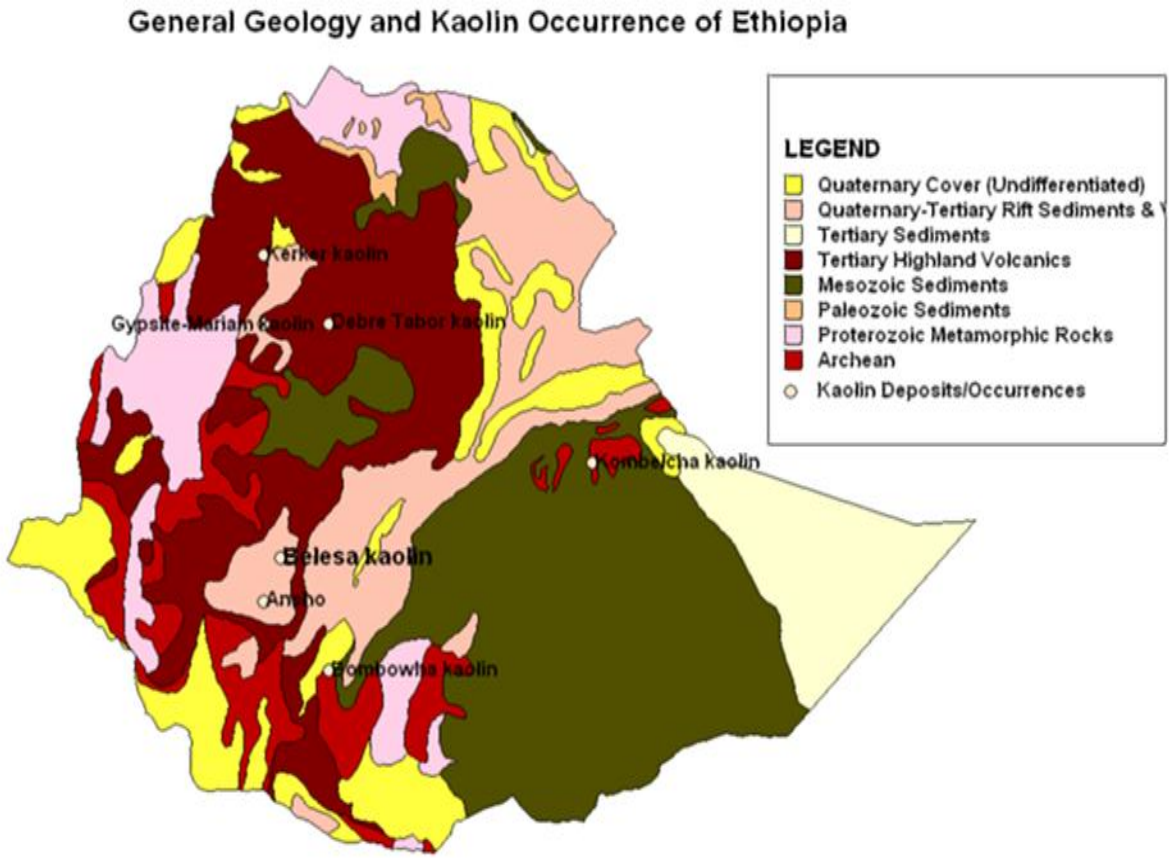

Figure 2.5:General Geology and Kaolin Occurrences of Ethiopia (Ayele et al. 2015)

The preparation of zeolites is generally expensive and, therefore, their use in environmental remediation is restricted due to prohibitive costs. Cost limitations can be overcome by using low-cost raw materials for zeolite synthesis, such as kaolin. Ethiopia has a large kaolin reserve (20 million tons) that is dispersed over the country, including Tigray, Amhara, Oromia, and Southern Nations, Nationalities (Zewdie et al. 2021) (figure 2.5). However, there is hardly any report on the synthesis of zeolite Na-X from Ethiopian kaolin. The present research will be concerned with the synthesis of zeolite Na-X from kaolin and its characterization using various techniques, and in the investigation of the lead ion removal capacity of the adsorbent from wastewater has been dealing with the use of the material for the removal of lead ion from wastewater.

2.3. Removal of Lead from Waste Water Using Adsorbents

In effluents and sewage from industries including paint, pesticides, batteries, mines, and smelting, lead (II) is frequently found. Fig. 2.6 shows the numerous environmental sources of Pb (II) pollution. Lead (II) toxicity causes many illnesses, including brain and kidney damage, severe stomachaches, hypertension, defective blood synthesis, and miscarriages in pregnant women. In addition, lead (II) is ubiquitous pollution on earth, and exposure to it through watery media results in weak ankles, fingers, and wrists. Fig. 2.6 depicts a few of the hazardous consequences of Pb (II) on people, animals, and plants. Biological systems are particularly at risk from lead (II) contamination. Because lead (II), along with cadmium and mercury, is the most hazardous heavy, metal contaminant (Bayuo, Rwiza, and Mtei, 2022a).

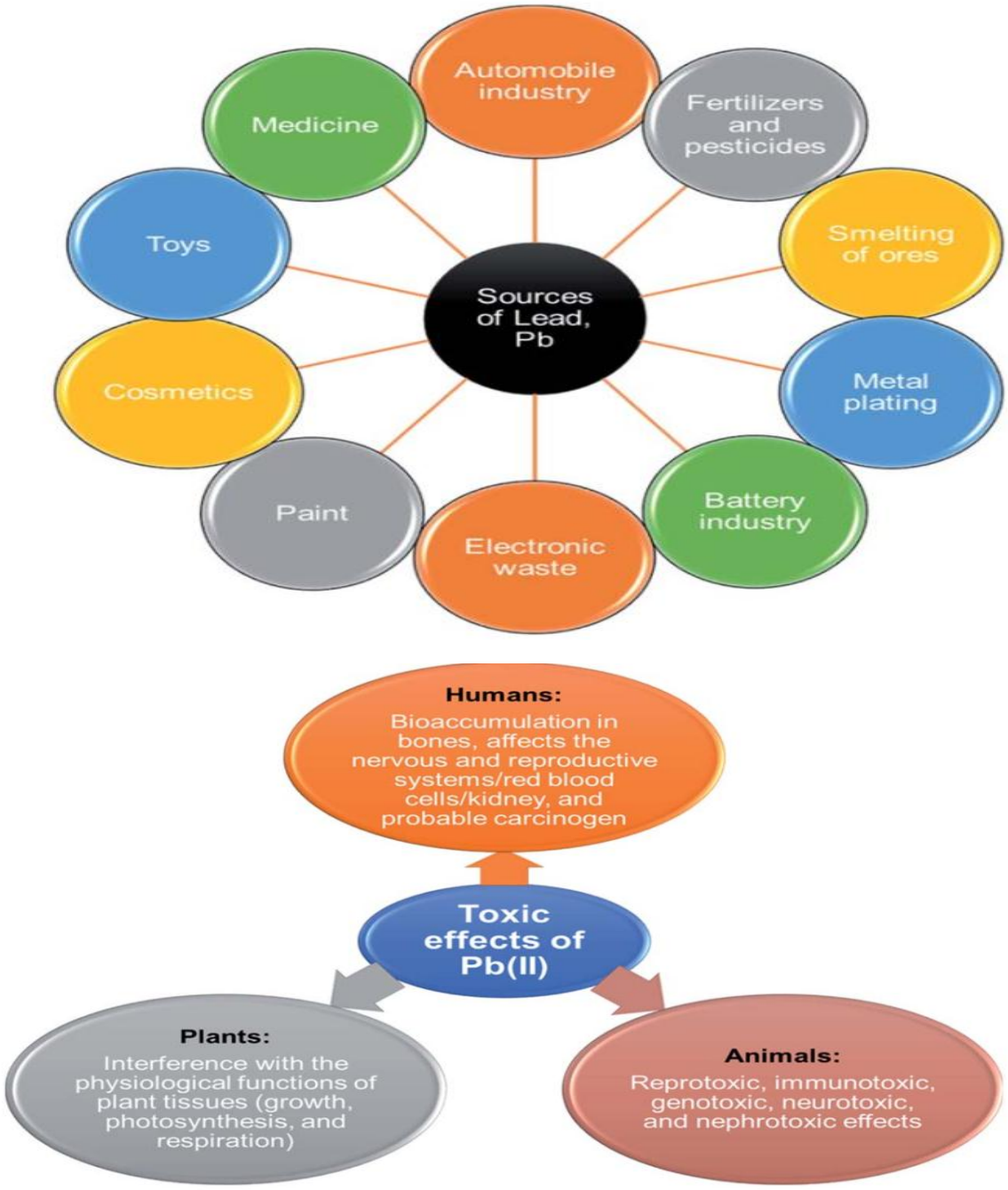

Figure 2.6. Various sources of Pb (II)ion pollution in the environment and its Toxic effects (Bayuo, Rwiza, and Mtei 2022)

Coagulation, precipitation, contact precipitation, electro-coagulation, electro-dialysis, reverse osmosis, solar distillation, adsorption, ion exchange, and other membrane technologies are conventional methods for removing metal ions from wastewater. However, most of these technologies are either utterly ineffective or too expensive for tiny firms, such as those found in

developing nations. For that reason, in recent years, environmental research has shifted its attention to the deployment of less expensive alternative technologies. The ideal removal of harmful metal ions from water requires the employment of inexpensive, powerful, secure, and adaptable media that may be used in a variety of wastewater situations.(Wambu et al., 2018). Many treatment systems have been probed for heavy metals reduction from wastewater and water; however, many of these management processes are significantly pricy and incompetent at eliminating low-level concentrations of heavy metals. In comparison, adsorption appears to be more resourceful and used worldwide owing to the greater yield and cost-effectiveness of the adsorbents (Khandanlou et al., 2015).

Adsorption methods for removing heavy metals continue to spur interest given their selectivity, low cost, ease of use, high efficiency (even when these metals are in low concentration), and the possibility of reusing the materials involved. Polymers, silica, nanocomposites, metal-organic frameworks (MOFs) supported on the nanofibrous membrane, and other materials such as activated carbon have all been studied as possible adsorbents (Jos et al., 2018).

2.4. Removal of Lead from Waste Water Using zeolites

Natural materials that are available in large quantities such as used in this research kaolin (zeolite) or specific waste from agricultural operations may have the potential to be used as low-cost adsorbents, as they represent unused resources, are inexpensive, require easy process, available and abundant in nature and are environmentally friendly (Rahman et al., 2022).

The zeolite-based made-up materials exhibit excellent ring-like complex features towards toxic substances, a rapid adsorption pace, and good reuse ability due to the synergistic action of inorganic/polymers and zeolites for the adsorption of pollutants from aqueous.(Roshanfekr Rad and Anbia, 2021)

The natural materials that remove lead (II) ions from an aqueous solution include natural clay, sand particles, peat moss, natural goethite, natural bentonite clay, chitin, and talc surface. The natural bentonite clay and acid-activated bentonite clay were reported to have the maximum adsorption capacity of 83.0 and 92.9 mg/g of lead ions, respectively. Impregnated activated carbon nanoparticles on the surface of the expanded lightweight clay aggregates and used them as adsorbents for Lead (II) ion removal. The maximum adsorption capacity was 22.8 mg/g,

which removed 99% of Lead (II) ions from a concentration of 100 mg/L with an adsorbent dose of 10 g/L(Rahman et al., 2022).

The zeolite N.P./PEG/GO nano-composite was successfully produced using a hydrothermal aided sol-gel process and characterized by FT-IR, XRD, SEM, and EDS. The nano-composite was utilized to remove Pb2+ and Cd2+ ions from water samples as the adsorption procedure's effective parameters, pH, contact duration, dose, and temperature were tuned. The results reveal that interference ions have no significant effect on the removal % of Pb2+ and Cd2+ ions by zeolite N.P./PEG/GO composite. The adsorbent capacity of Pb2+ and Cd2+ions was 49.6 and 50.2 mg ion per gram adsorbent, respectively(Samadi, Shalmani, and Zakaria 2019) .

A reversible chemical process called "ion exchange" is employed to swap out dangerous metal ions for healthy, environmentally friendly ones. By bonding a heavy metal ion to an immobile solid particle in place of the solid particle cation, one can remove heavy metal ions from the wastewater solutions. Solid ion-exchange particles' constituent materials might be either synthetic (like organic resins) or natural (like inorganic zeolites). Pb^{2+}, Hg^{2+}, Cd^{2+}, Ni^{2+}, V^{4+}, V^{5+}, Cr^{3+}, Cr^{4+}, $Cu^{2+,}$ and Zn^{2+} are a few examples of heavy metal ions that the ion-exchange method may be able to remove from wastewater (Qasem, et.al. 2021).

Cations are removed using several sorts, such as Amberlite115 and Diaion CR11116. Because of its negative charge caused by Si4+, which lies in the center of the tetrahedron and undergoes isomorphous replacement with Al3+ cations, zeolite has a strong ion exchange capacity. MOFs have lately been proposed as potential candidates for the ion exchange removal procedure (Qasem, Mohammed, and Lawal, 2021).

Despite raw zeolites' outstanding adsorption ability, the primary problems with the zeolites utilized in the adsorption operation are the difficult zeolite separation from the watery solution and the increased pressure dip in the fixed-bed column. Recently, zeolite/inorganic and zeolite/polymer combinations have been developed, both of which are effective water adsorbents. Zeolite-based composites have attracted a lot of attention from researchers in recent years for the adsorption process due to their superior physicochemical equilibrium, ease of reusability, and higher ability to adsorb as compared to raw zeolites. Furthermore, adding zeolite

to polymers as a filler might improve the durability of polymeric adsorbents. The efficacy of clay-based products has lately been called into question (Roshanfekr Rad and Anbia, 2021).

Pb (II) showed the maximum ability to adsorb all of the heavy metals (27.70 mg/g for chloride-modified zeolite, 113 mg/g for Fe-modified zeolite, 653 mg/g for surfactant adjustable zeolite, 808 mg/g for synthesized zeolites, and 909.09 mg/g for nano zeolite). Other heavy metals with strong adsorption capacities on synthesized zeolites consisted of Cr(IV), Cu(II), Ni(II), Zn(II), and Co(II) (Malakootian, Nouri, and Hossaini, 2009)(Irannajad and Kamran Haghighi, 2021).

The elimination of Cd 2+ and Pb2+ from zeolite as a consequence of concentration was examined at constant temperature (30 0.1 C) by adjusting the metallic concentration from 100 to 600 mg/L while holding all other parameters constant. The percentage adsorption of Cd 2+ and Pb 2+ decreases with increasing metal content in aqueous solutions. These findings imply that when metal content in the aqueous solution increases, energetically less favorable locations become involved. The maximum exchange values achieved were as follows: Cd 2+ 55%, Pb 2+ 96% (Sayed and Khater 2013)

The hydrothermally assisted sol-gel technique was used to effectively synthesize the zeolite N.P./PEG/GO nano-composite, which was then analyzed by FT-IR, XRD, SEM, and EDS. The nano-composite was utilized to remove Pb2+ and Cd2+ ions from various water samples. As effective parameters in the method of the adsorption process, the pH, contact duration, dose, and temperature were tuned. The results showed that the presence of interference ions has no significant effect on the removal % of Pb2+ and Cd2+ ions by the zeolite N.P./PEG/GO composite. Pb2+ and Cd2+ion adsorbent capacities were 49.6 and 50.2 mg ions per gram of adsorbent, respectively (Samadi et al., 2019).

3. MATERIALS AND METHODS

3.1. Chemicals

The following chemicals were used: Sodium hydroxide anhydrous pellets (NaOH 99% Sigma Aldrich), Lead (II) nitrate (Pb $(NO_3)_2$ 99%, CDH), hydrochloric acid (35% from institute lab), distilled water, powder of kaolin from Hawassa was used in this experiment.

3.2. Instruments and Apparatus

Other materials and instruments that were used include polyethylene bags, conical flasks, measuring cylinders (different sizes), filter paper (grade 1 diameter 90 □m), orbital shaker, spatula, pipettes, aluminum sheet, beakers (different sizes), Sieve 200 mesh, thermometer, pH meter (HANANA, Model HI-991301, USA), Analytical balance (LA114, Japan), Desiccators, Muffle furnace, Glass stirring rod, Mortar and pestle, water bath, Powder X-Ray diffract meter (XRD, Bragg-Brentano geometry with Cu-Kα radiation at 30 mA and 40 kV. Data collection was carried out in the 2θ range 10-90°, at a scanning speed of 100 per minute and scanning step of 0.05°), Scanning electron microscope (SEM, JCM-6000 plus, SM-MAGKEY 600X, 15 KV), surface area analysis BET (Horiba instruments, Inc., SA-9600 series surface area analyzer), Atomic absorption spectroscopy (AA 2400FS Varian), centrifuge (U8V-2LWSCIENTFIC LTD, UK), Oven for drying were used during this work. The kaolin, meta-kaolin, and synthesized zeolite-x were characterized by powder XRD, BET, FTIR, and SEM.

3.3. Synthesis of Zeolite Na-X from Kaolin

The raw kaolin precursor was collected from Hawassa, Tabor Hill, and southern Ethiopia. The natural kaolin was washed with distilled water to remove irrelevant matter and dried to remove the moisture in an oven at 100oC for 24 h. Powder preparation techniques using a mortar and pestle were carried out. After grinding, samples were sieved under dry conditions, and the smallest of the collected particles (less than 75 μm)(Aragaw and Ayalew 2019) used for uniform in size and formed high-quality and pure crystalline zeolite was formed(Rodrigues, Souza, and Santos, 2016) was selected for zeolite-X synthesis.

In this study, an alkaline fusion step before treatment was adopted with a bit of modification because it plays an important role in enhancing the conditions for zeolite synthesis and because larger amounts of aluminosilicate can be dissolved. In a typical synthesis process, 68.2 g of the raw material was dry mixed with 81.8 g of NaOH in a raw material/alkaline activator ratio = 1/1.2 in weight for 30 min to a uniform solution and the resultant mixture was fused at 600 °C for 1 h(Bai et al., 2018). The alkaline reagent that was added to the starting material acted as an activator during fusion. Some of the source materials' inert crystalline phases can be completely reacted. To generate the amorphous precursors, the fused product was pulverized in a mortar and pestle and then dissolved in 236.5ml of distilled water (ratio 1/4.9) under stirring circumstances. The reaction was carried out under static circumstances and heated to 100°C for 1 hour. And hydrogels were aged for 24 hours under static circumstances (Medina-Rodrguez et al., 2021). Then, the reaction mixtures were filtered and washed with distilled water to remove excess alkali until the pH of the filtrate dropped below 10 (Cooper, Doucet, and Pratt, 2007). Finally, the samples were oven-dried at 80 °C overnight. The dried samples were weighed and kept in plastic bags for characterization (Medina-Rodríguez et al., 2021).

3.4. Adsorption Experiments

In the field of adsorption, adsorption performance can be expressed as the amount of adsorbate adsorbed at equilibrium or the percentage of the removed adsorbate. The standard stock solution of lead was prepared by dissolving 1.615 g of 99% analytical grade Pb (NO3)2 in 1000 mL of distilled water. Synthetic samples of different lead concentrations were prepared from this stock solution by diluting it with distilled water to obtain the desired concentration. The pH of the aqueous solution was adjusted to the desired value by adding 0.1 M HCl or 0.1M NaOH

3.5. Experimental Design

Response surface methodology (RSM) is one of the powerful statistical experimental design techniques applied to build models and investigate individual and interaction effects of the selected operating condition on the given response in a given experiment. It is a very practical approach for the optimization of complex processes in a more convenient way resulting in saving time, labor, and cost. Box–Behnken design (BBD) is one kind of RSM, which helps to design a second-order response model. BBD can provide a maximum amount of complex information

with minimum experimental time. Furthermore, in comparison with other statistical methods, such as full factorial design, it requires a few numbers of runs. Most importantly, it avoids the analyses at their extreme combinations (such as at the highest and lowest levels) for which unsatisfactory results might occur (Kassahun et al., 2017). RSM, on the other hand, is an empirical modeling method for identifying the interaction between various operation factors and response variables. Furthermore, it is a set of mathematical and statistical approaches for modeling and evaluating issues in which the response is influenced by a wide range of operational factors, the effects of which are difficult to separate. RSM, in general, provides a sequential experimental technique for developing and optimizing empirical models (Gebregziabher et al, 2021). Design Expert version 13.0.1, a statistical program, was used to examine the trial data. BBD created Equations for regression analysis as well as statistical significance evaluation.

3.5.1. Batch Adsorption Experiment

In a batch system, the performance of the zeolite (Na-X) in the adsorption of lead ions from an aqueous solution was examined as a function of pH, contact time, adsorbent dosage, and starting metal concentration. The effects of adsorption operating parameters such as lead concentrations, contact time, pH, and the synthesized zeolite-X were investigated in a 100 mL conical flask containing 100 mL of distilled water on a rotary shaker with a constant agitation speed of 250 revolutions per minute (rpm) at room temperature of 22 2oC. 0.1 M HCl / 0.1 M NaOH solutions were used to modify the pH of the solutions.

The optimum adsorption condition was determined by conducting a series of experiments according to BBD as shown Table 3.2.

Table 3.1. Experimental levels of selected variables for BBD

Name	**Units**	**Low**	**High**	
contact time	Min	15	90	(Hussain et al. 2021)
Mass .of adsorbent	g	0.5	5	(Pandey, Sharma, and Sambi 2015)
Conc. of lead	mg /L	1	30	(Pandey et al. 2015)
pH		3	9	(Dawagreh, Hailat, and Alkhasawneh 2017)

Table 3.1 shown the reason why the four parameters are chosen? Because they mainly affect adsorption, that is, pH, is necessary to identify in which zone it adsorbs and, at the same time, what kind of concentration it acts on. Beyond that, we know that if there is an amount that can be removed, on the other hand, time is also important, as is their value. I chose the values of each parameter because it allows you to see the change in small amounts by looking at previous research.

Table 3.2. Batch adsorption factors and the effect of removal of Pb (II)

SDT	Run	Factor 1 Contact time (min)	Factor 2 Mass adsorbent (g)	Factor 3 Conc. of Pb (II) ion(mg/L)	Factor 4 pH	% Removal Efficiency
3	1	15	5	15.5	6	
4	2	90	5	15.5	6	
26	3	52.5	2.75	15.5	6	
2	4	90	0.5	15.5	6	
23	5	52.5	0.5	15.5	9	
18	6	90	2.75	1	6	
5	7	52.5	2.75	1	3	
21	8	52.5	0.5	15.5	3	
29	9	52.5	2.75	15.5	6	
22	10	52.5	5	15.5	3	
13	11	52.5	0.5	1	6	
28	12	52.5	2.75	15.5	6	
11	13	15	2.75	15.5	9	
16	14	52.5	5	30	6	
27	15	52.5	2.75	15.5	6	
15	16	52.5	0.5	30	6	
9	17	15	2.75	15.5	3	
14	18	52.5	5	1	6	
8	19	52.5	2.75	30	9	
17	20	15	2.75	1	6	
1	21	15	0.5	15.5	6	
25	22	52.5	2.75	15.5	6	
20	23	90	2.75	30	6	
10	24	90	2.75	15.5	3	
7	25	52.5	2.75	1	9	
6	26	52.5	2.75	30	3	
19	27	15	2.75	30	6	
24	28	52.5	5	15.5	9	
12	29	90	2.75	15.5	9	

The remaining concentration of Lead (II) ion in each sample after adsorption at different time intervals was determined by atomic absorption spectroscopy (AAS) after filtering the adsorbent

with grade 1 filter paper to make it adsorbent free. The amount of the lead ion adsorbed q_t and q_e was calculated as follows according to the following equation:

$$\mathbf{q_t} = \frac{\mathbf{V(C_0 - C_t)}}{\mathbf{1000M}} \quad \textbf{(1)}$$

$$\boldsymbol{q_e} = \frac{\boldsymbol{(C_0 - C_e)V}}{\boldsymbol{1000M}} \quad \textbf{(2)}$$

Where q_e and q_t are adsorption capacities (mg g^{-1}) of the lead ion at equilibrium and at any time, respectively. And C_0, C_t, and C_e are initial concentrations, and equilibrium concentrations of the lead ion in aqueous solutions (mg L^{-1}) respectively, V is the volume of the solution (mL), and M is the mass of the dry adsorbent (g). The percentage of lead ions removed was obtained from equation (3)

$$\%\boldsymbol{Removal} = \frac{\boldsymbol{(C_0 - C_e)}}{\boldsymbol{C_0}}\boldsymbol{x100} \quad \textbf{(3)}$$

Where, % Removal was the ratio of the difference in lead concentration before and after adsorption(Woldeamanuale 2017).

3.6. Adsorption Isotherms

Many isotherm models are frequently used to fit the adsorption equilibrium data to get a linear regression to predict the maximal sorption capacity of the employed adsorbent. In most of the numerous studies reviewed, the adsorption processes were justified by applying linear forms of one-parameter adsorption isotherm model (Henry), two-parameter adsorption isotherm models (Langmuir, Freundlich, Dubinin–Radushkevich, Temkin, Harkin–Jura, and Elovich), and three-parameter adsorption isotherm models(Bayuo, Rwiza and Mtei, 2022b).

In this research, Adsorption models like Langmuir and Freundlich isotherms are frequently employed in most adsorption research to assess adsorption processes. In general, data from experiments were fitted to adsorption isotherm models, and then equilibrium adsorption was explained using the best-fit model. The most suitable adsorption model was chosen only two models i.e. Langmuir and Freundlich were selected and used.

Because of their simplicity, adaptability, and application to a wide range of adsorption systems, Langmuir and Freundlich's adsorption isotherm models are commonly selected over others. This

is why: Because it implies monolayer adsorption on a homogenous surface, the Langmuir model is generally favored for systems with a limited number of identical adsorption sites. It gives useful insights into the maximum adsorption capacity and equilibrium constant, both of which are critical characteristics for understanding adsorption processes.

The Langmuir model is particularly useful when the adsorbate-adsorbent interaction is strong and the adsorption occurs on a single layer. The Freundlich model is highly preferred when dealing with heterogeneous surfaces and non-ideal adsorption systems. It offers more flexibility as it accounts for variations in adsorption capacity with the concentration of the adsorbate(Song et al. 2013).

The Freundlich isotherm equation provides information about the adsorption intensity (Freundlich constant) and adsorption non-linearity (Freundlich exponent). This model is particularly useful when the adsorbent surface has varying affinity and the adsorption process is not limited to a monolayer. While other models like Dubinin–Radushkevich, Temkin, Harkin–Jura, and Elovich have their own merits and applications, Langmuir and Freundlich models are preferred due to their simplicity and wide applicability. These models have been extensively studied and validated, making them reliable tools for adsorption analysis. However, it's important to note that the choice of the most suitable model depends on the specific adsorption system and the nature of the adsorbate-adsorbent interaction. It is always recommended to consider multiple models and compare their goodness-of-fit to the experimental data to ensure accurate characterization of the adsorption process.

3.6.1. Langmuir Isotherm

The Langmuir isotherm of monolayer adsorption. Irving Langmuir published the knowledge on adsorption between gases and solids. The isotherm formula is built on the following hypotheses. A monolayer was formed at the highest adsorption process: (a) similar surfaces of the adsorbent material are collected; (b) molecules of the adsorbent material do not attract one another; (c) uniform mechanisms of adsorption; and (e) molecules of the adsorbate are adsorbed at the open area of the adsorbent.(State et al. 2020).

The above-mentioned theory, which states that there was no attraction between the adsorbed metals and the maximum adsorption occurs in a monolayer of adsorbent materials, led to the

development of the Langmuir isotherm model. The linear form of Langmuir isotherm models is given in Equation

$$\frac{C_e}{Q_e} = \frac{C_e}{Q_e} + \frac{1}{K_L} Q_m \qquad \textbf{(4)}$$

Where "Ce" is the amount of Pb (II) (mg/L) at equilibrium, "Qe" is the uptake capacity (mg/g), while Qm is the possible monolayer coverage of the adsorbent (mg/g) and K_l is the Langmuir constant (L/mg) that specifies the adsorption energy. The slope and intercepts of the line of of "$\frac{C_e}{Q_e}$" vs "Ce" were used to compute the values of K_L and Q_m, respectively. The main characteristics of the Langmuir isotherm may be stated in terms of the equilibrium parameter R_L, which is a dimensionless constant known as the separation factor or equilibrium parameter.

$$\mathbf{R_L} = \frac{1}{1+(1+K_L C_0)} \qquad \textbf{(5)}$$

Where: C_0 = initial concentration

K_L = the constant related to the energy of adsorption (Langmuir Constant).

$$K_L = \frac{1}{Qm}, \qquad \textbf{(6)}$$

$$Q_m = \frac{1}{intercept} \; ; \qquad \textbf{(7)}$$

R_L value indicates the adsorption nature to be either unfavorable if R_L>1, linear if R_L =1, favorable if 0< R_L<1, and irreversible if R_L=0.(Mustapha et al. 2019)

3.6.2. Freundlich Isotherm

The Freundlich isothermal model explains the reversible and multilayer uptake of adsorbate for heterogeneous adsorption mechanisms. This can be defined as

$$\mathbf{q_e = K_f\ C_e^{1/n}} \qquad \textbf{(9)}$$

Can be written as, $\mathbf{Log\ q_e = log\ k_f + \frac{1}{n} log\ C_e}$ **(10)**

Where, q_e= mass of adsorbate adsorbed per unit mass of adsorbent, mg/g.

K_f = Freundlich capacity factor

C_e = equilibrium concentration of adsorbate in solution after adsorption, mg/L

1/n= Freundlich intensity parameter (Mabuza, Premlall, and Daramola 2022)

The values of "n" and "K_f" can be calculated from the slope and intercept of the linear plot of "log q_e" versus "log C_e".

3.7. Adsorption Kinetics

The kinetic data gathered in this work was fitted to the pseudo-first-order (zeolite x) and pseudo-second-order (zeolite x) models to look into the mechanism governing the adsorption processes.

The adsorption rate was dependent on the adsorption capacity, according to the pseudo-first-order model. The adsorption was thought to be regulated by a chemisorption process, which involves valence forces through electron sharing or transfer between the adsorbent and adsorbate. This was the foundation of the pseudo-second-order model(Tsvetanova et al. 2022).

To obtain a better understanding of the adsorption mechanism, the pseudo-first-order and pseudo-second-order models were used. The pseudo-first order model is the first model that describes the adsorption rate based on adsorption capacity. The pseudo-first-order model is generally expressed by

$$\mathbf{ln\,(qe - qt) = lnqe - K_1 t} \qquad \mathbf{(8)}$$

Where K_1 (min $^{-1}$) is the pseudo-first-order rate constant and q_e and q_t are the amounts of adsorption (mg/g) at equilibrium and time t (min)(Cordova Estrada, Cordova Lozano, and Lara Díaz 2021). The pseudo second-order kinetic model pro-posed is expressed in a linear form by

$$\mathbf{\frac{t}{qt} = \frac{1}{K_2} q_e^2 + \frac{t}{q_e}} \qquad \mathbf{(9)}$$

Where q_t is the amount of adsorption time t (min); $\mathbf{k_1}$ is the rate constant of first order reaction; $\mathbf{k_2}$ (g/[mg. min]) is the pseudo-second-order rate constant and $\mathbf{q_e}$ is the amount of adsorption equilibrium (mg/g)(Cordova Estrada et al. 2021).

4. RESULTS AND DISCUSSION

4.1. Characteristic of Zeolite-X Synthesized from Kaolin

Figure 4.1a as showed below the sample of collected kaolin dried in the sand, figure 4.1b showed that after calcination of kaolin to form meta-kaolin, and figure 4.1c showed the synthesized zeolite x which was crystalline white in color by mixing of sodium hydroxide.

a

b

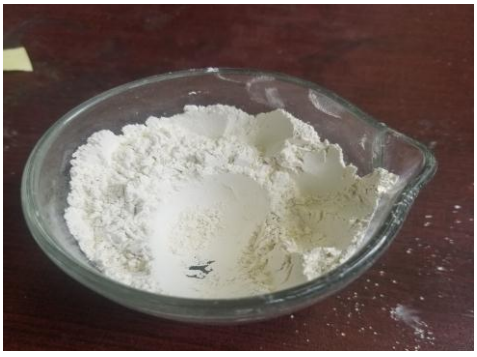

c

Figure 4.1 a mineral kaolin, b meta-kaolin and c synthesised zeolite-X

4.1.1. XRD Patterns Analysis

The analysis of X-ray diffraction (XRD), a non-destructive technique, can provide exact information on a material's crystallographic structure, chemical composition, and physical properties. At ambient temperature, three samples were examined using X-ray diffraction (XRD). This search and match function indicated the presence of other phases, such as quartz in

all the 3 samples as shown in Fig. 4.2 shows XRD peaks showing the typical diffraction pattern of Kaolin (Fig.4.2a), meta-kaolin (Fig.4.2b) and Zeolite-X (Fig.4.2c).

The XRD patterns of meta-kaolin and kaolin can show both similarities and differences, indicating the structural changes that occur during the transformation from kaolin to meta-kaolin. Similarities: Presence of quartz peaks: Both meta-kaolin and kaolin can exhibit peaks corresponding to quartz, which is a common impurity found in these minerals. The presence of quartz peaks in the XRD patterns indicates that quartz is present in both meta-kaolin and kaolin samples. Differences: Crystalline peaks: Kaolin typically shows characteristic peaks corresponding to its crystallographic structure, such as peaks at angles around 14.5°, 25.22°, and 35.9 ° (2-theta). These peaks represent the crystal planes of kaolinite, the primary mineral in kaolin. In contrast, meta-kaolin may exhibit a loss or significant reduction in these crystalline peaks at angle around, 21.07°, 24.04°, 26.92°, 27.94°, and 29.72° (2-theta). Indicating a change in the crystal structure due to the activation process. Amorphous nature: Meta-kaolin, after undergoing activation or calcination, can exhibit an amorphous nature. This means that the XRD pattern of meta-kaolin may show a lack of distinct crystalline peaks, indicating a disordered or non-crystalline structure. This is in contrast to kaolin, which typically exhibits well-defined crystalline peaks. Additional phases: The XRD pattern of meta-kaolin may show the presence of additional phases or compounds that are not present in kaolin(Irfan Khan et al. 2017).

The activation process results in the synthesis of zeolite-X compounds, the XRD pattern of meta-kaolin may exhibit peaks corresponding to these new phases. In summary, while both meta-kaolin and kaolin may exhibit peaks corresponding to quartz, there are notable differences in their XRD patterns. Meta-kaolin may show a loss of crystalline peaks, an amorphous nature, and the presence of additional phases resulting from the activation process. These differences indicate the structural changes that occur during the transformation from kaolin to meta-kaolin.

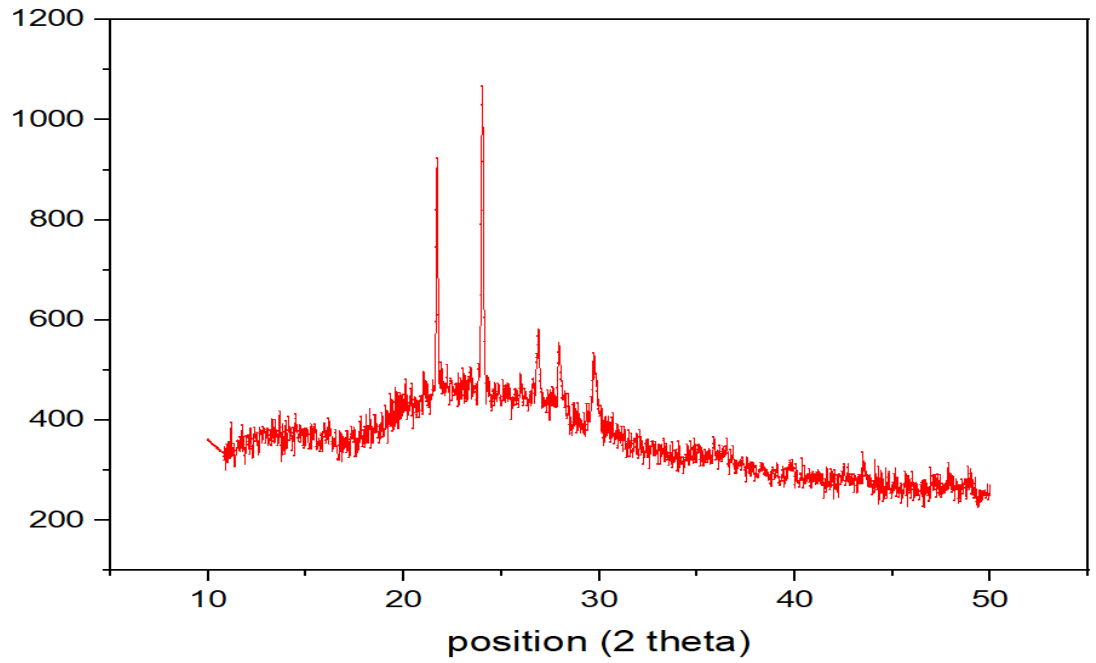

Figure 4.2 a. XRD pattern of Kaolinite

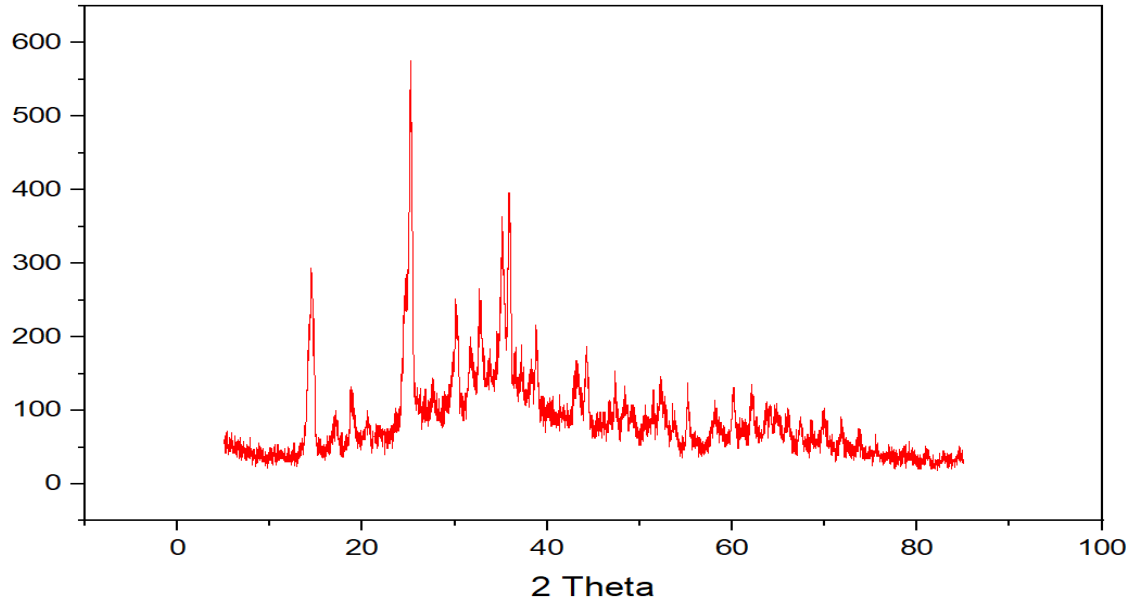

Figure 4.2b XRD pattern of Meta-Kaolinite

Figure 4.3 shows the X-ray powder diagrams as a result of the manufactured zeolite-x material diffractogram. The XRD pattern of Zeolite X typically exhibits a series of characteristic peaks at specific 2θ values, indicating its unique crystallographic structure. The specific peak positions may vary slightly depending on the sample preparation and other experimental conditions. Here is an explanation of the peaks you mentioned = 14.26°: This peak corresponds to a specific crystal plane in Zeolite X, representing a characteristic feature of its crystal structure.2θ = 18.8°: Another peak associated with a particular crystal plane in Zeolite X.2θ = 24.5°: This peak corresponds to yet another crystal plane in Zeolite X, contributing to its unique XRD pattern.2θ = 25.1°: Another peak indicating a specific crystal plane in Zeolite X.2θ = 26.08°: This peak represents a crystallographic feature of Zeolite X.2θ = 30.04°: A distinct peak associated with a particular crystal plane in Zeolite X.2θ = 31.16°: Another peak contributing to the XRD pattern of Zeolite X.2θ = 32.64°: This peak represents a crystallographic feature of Zeolite X.2θ = 35.84°: A prominent peak indicating a specific crystal plane in Zeolite X.2θ = 38.08°: Another peak contributing to the XRD pattern of Zeolite X,2θ = 43.08°: This peak represents a crystallographic feature of Zeolite X.2θ = 47.28°: Another distinct peak associated with a particular crystal plane in Zeolite X. These peaks collectively form the XRD pattern of Zeolite X, providing information about its crystal structure and composition. The specific positions and intensities of these peaks are characteristic of Zeolite X and can be used for its identification and characterization similar to earlier literature (Kwakye-Awuah et al. 2016).

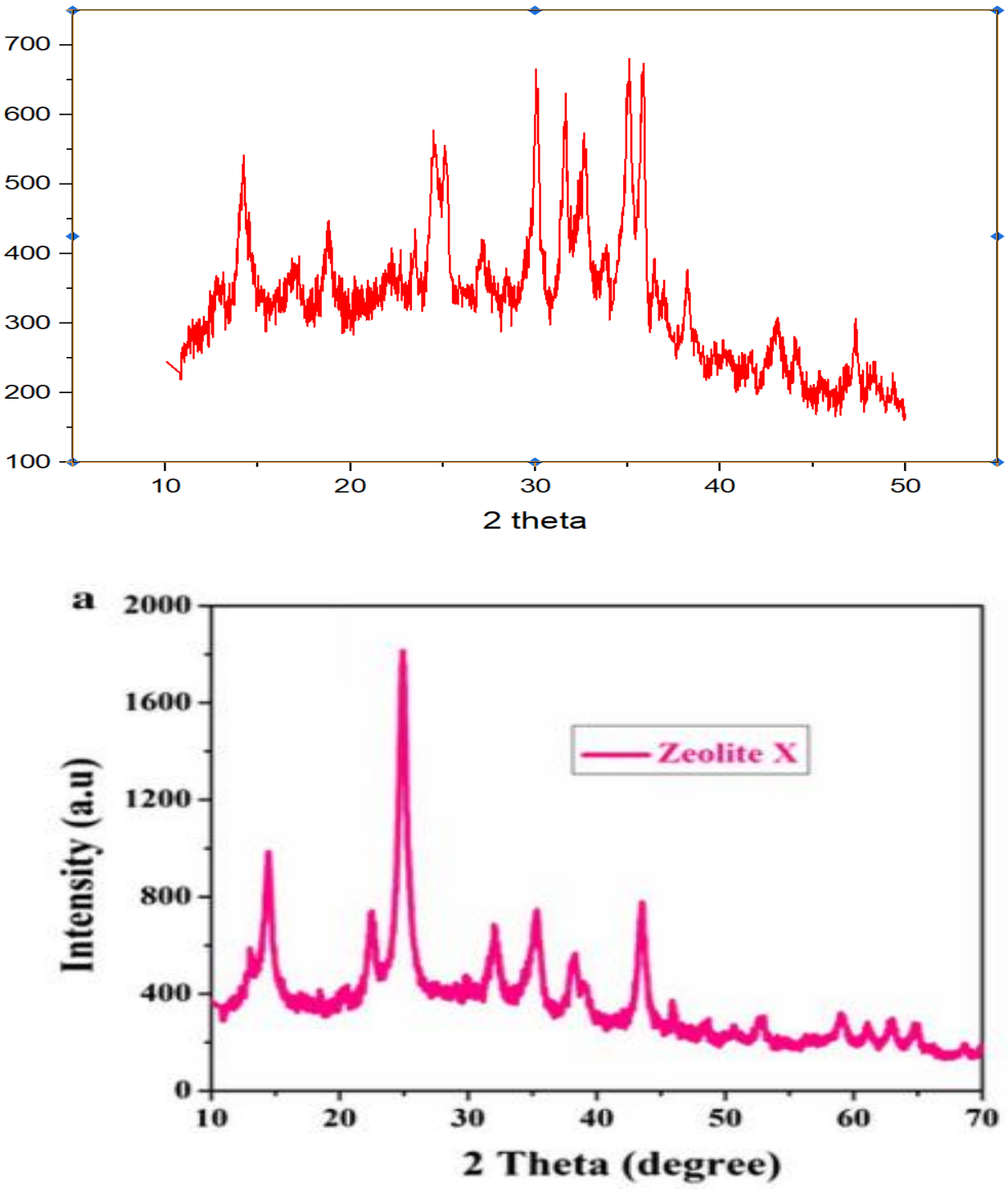

Figure 4.3. The XRD Patterns, Synthesized zeolite-X and reference zeolite-X(Na-X)(Fanta et al. 2019)**.**

4.1.2. SEM Observations of Kaolin, Meta-kaolin, and Zeolite-X

The SEM device characterized surface morphology pictures of the kaolin, meta-kaolin, and zeolite-X materials. With 5 µm, 10 µm, 20 µm, and 50 µm porous diameters as the operating parameters, the equipment was utilized to scan the surface morphology of materials for images of particles at different magnifications. The SEM parameters used in this study were appropriately matched by Zewdie et al. (2021). The SEM image (Fig. 4.3a) showed the existence of huge particles that looked like they were made up of several flaky particles packed together to produce a compact arrangement in hexagonal shapes, irregular bulk edges, and surfaces. Kaolinite-calcinated kaolin has a flattened platelet structure and is made up of homogeneous, transparent, and small-flake-shaped particles. Fig.4.3b showed that the meta-kaolin particles were plate-like in shape and occur both individually and as agglomerates. The size of a single meta-kaolin particle hardly exceeds 20 µm and 50 µm. The edges of the particles can be either sharp or rounded.

The SEM images of zeolite-x (Figure 4.4c) reveal that the sample is porous. The outer surface area of crystalline zeolite particles with sizes ranging from 5 to 20 micrometers constitutes just a small percentage of the total surface area. As a result, the bulk of active sites are situated within the pores. The geometrical link between the pores and the form of the molecules effects the rate and selectivity of reactions for molecular reactants or reaction products with sizes corresponding to the zeolite pore size. This characteristic, known as molecular filtering or shape selectivity, is one of the most essential aspects of zeolites.(Yokoi 2016) The picture is formed by the presence of clusters, and their particle aggregation on the sample's surface. A closer look group cluster revealed that its surface was covered in grains of all sizes and shapes. Three distinct types of grain forms can be identified: cubic, rectangular, and irregular (Pandiangan et al., 2017). The morphologies confirm the phase purity of the Zeolite (Na-X), which had an octahedral crystal structure, similar to those of the known literature. The images indicate that the prepared material consists of crystallites having an octahedral morphology with sharp edges expected of zeolite-X (Na-X)(Derbe, Temesgen, and Bitew, 2021).

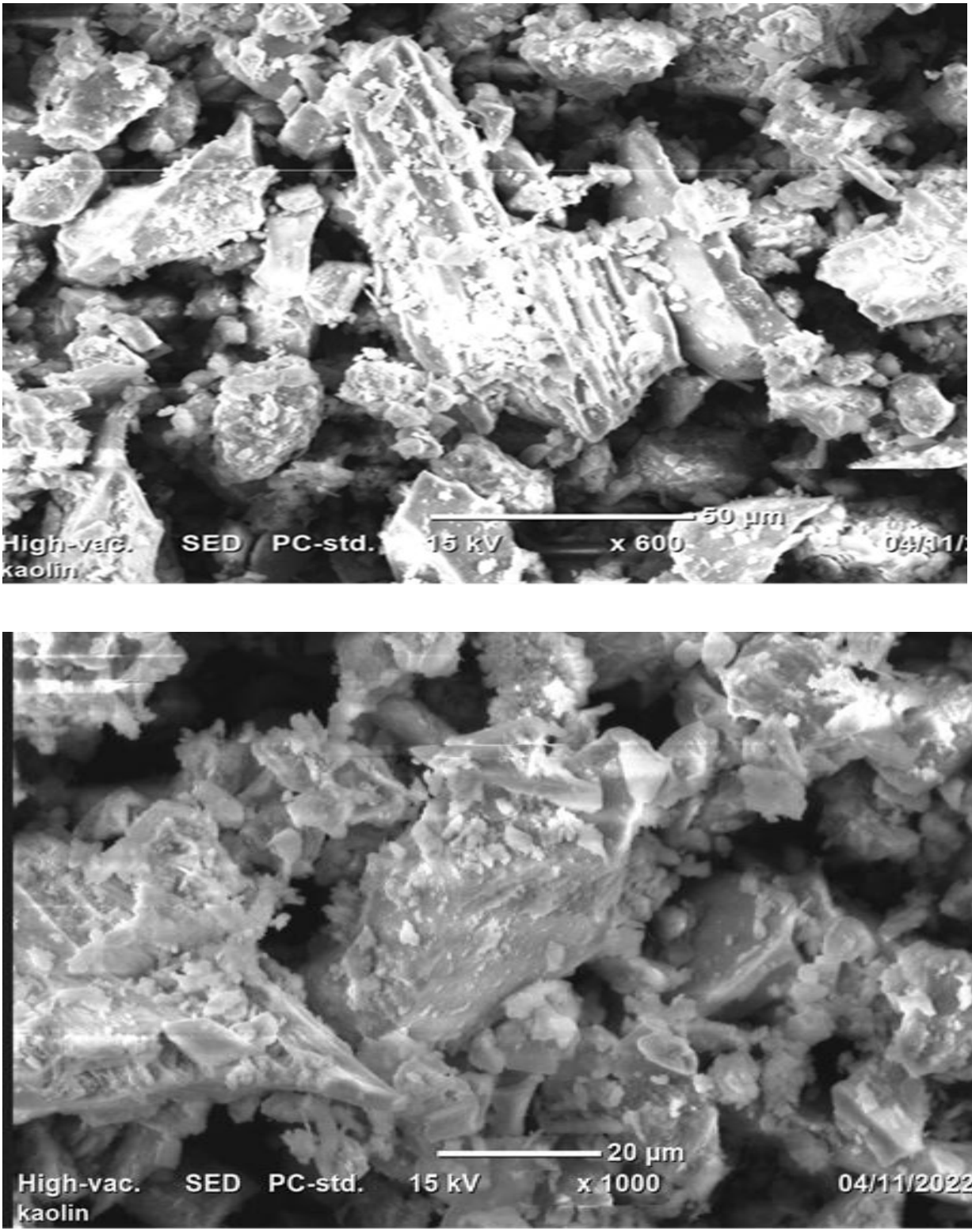

a) SEM image of kaolinite

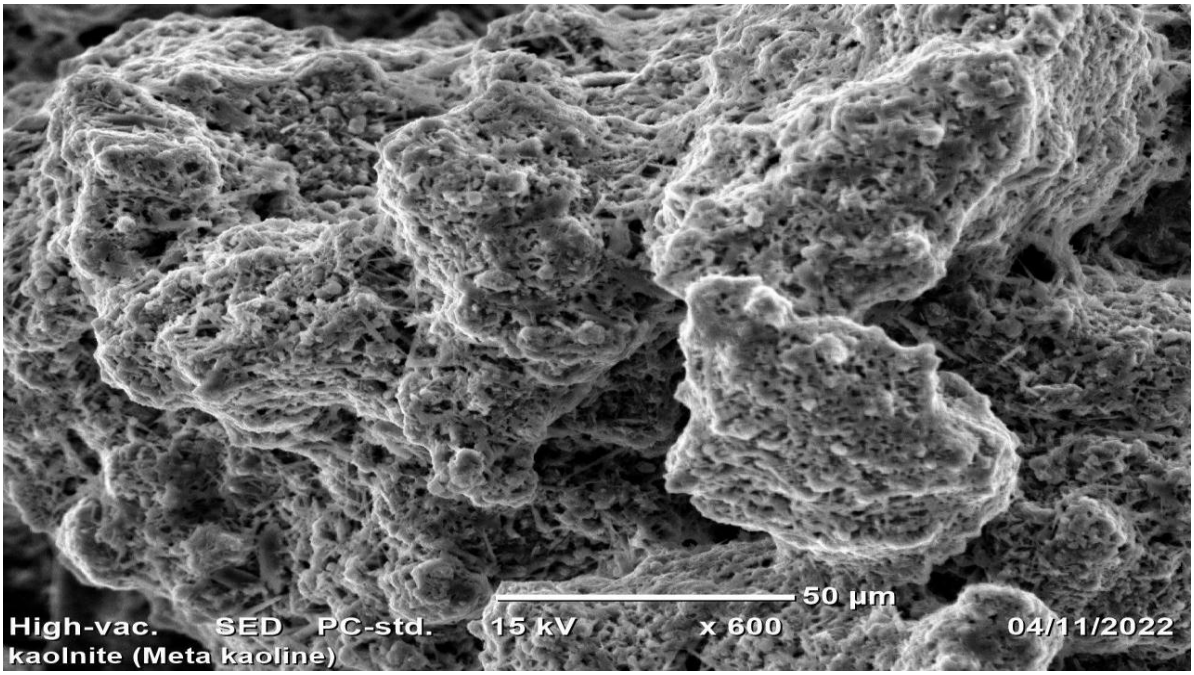

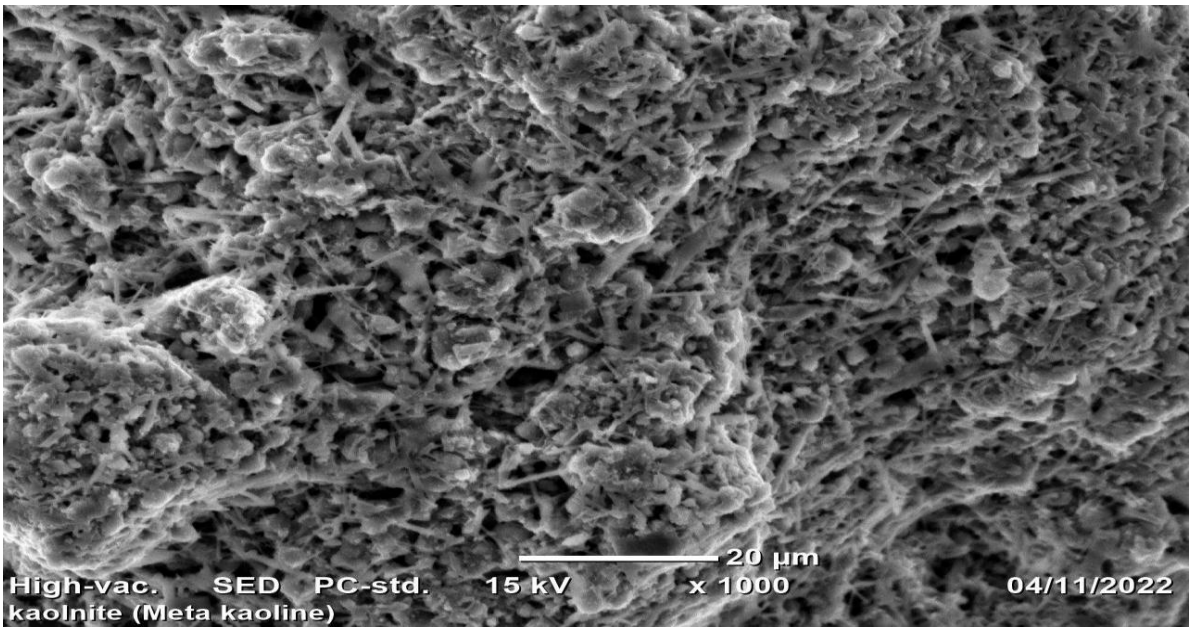

b) SEM image of Meta-kaolinite

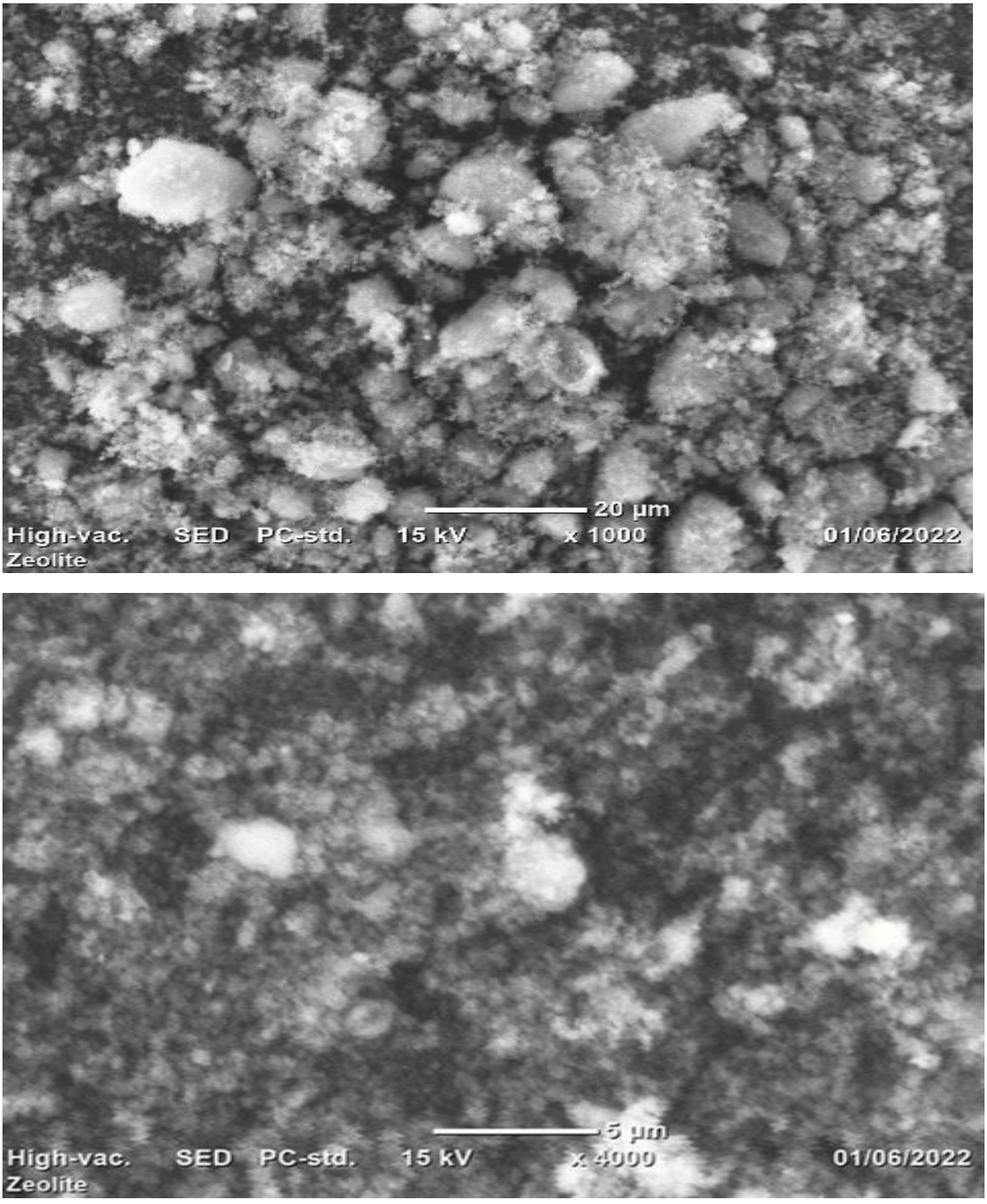

c) SEM image of Zeolite-X

Figure 4.4: Scanning Electron Micrograph (SEM) of kaolinite, meta-kaolinite and the synthesized zeolite-X (Na-X)

4.1.3. BET Results Analysis

The BET technique is used for calculating the particular area of the surface of porous materials, both amorphous and crystalline. A minimum of five data points in the P/P0 range of 0.025 - 0.30 should be utilized to correctly compute a surface area using a BET equation. Capillary condensation begins at pressures greater than 0.5, although at low pressures, only monolayer formation occurs. The N2 adsorption-desorption method was used to evaluate the surface characteristics of the synthetic zeolite-X, as illustrated in Figures 4.5 a and b. The zeolite-X isotherm was typed with a type H3 hysteresis loop. The strong adsorption at relatively low pressures (P/P0 0.1) indicated the presence of a porous structure. The BET surface area of the synthetic zeolite-X (Na-X) and the precursor kaolinite and meta-kaolinite is shown in Table 4.1. The BET surface area of synthetic zeolite-X was 57.94 $m^2 \bullet gm^{-1}$, whereas kaolin and Meta kaolinite have surface areas of 30.878 $m^2 \bullet gm^{-1}$ and 3.340 $m^2 \bullet gm^{-1}$, respectively. The BET study revealed that the synthetic zeolite-X had an excellent surface area that was bigger than that of kaolin and meta-kaolinite, allowing it to be used in adsorptions (Olaremu et al. 2018).

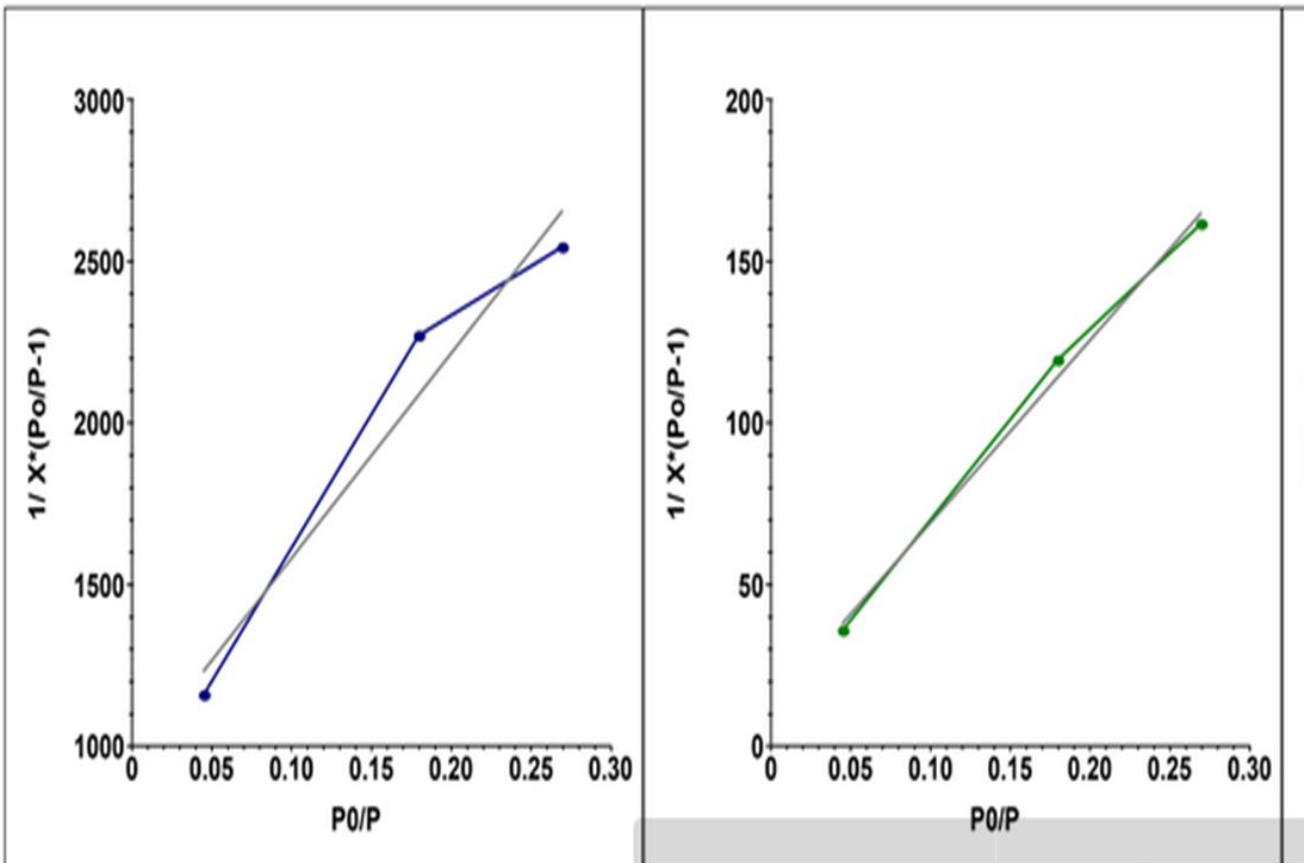

Figure 4. 5a. N2 adsorption-desorption isotherms of the kaolin and Meta kaolin

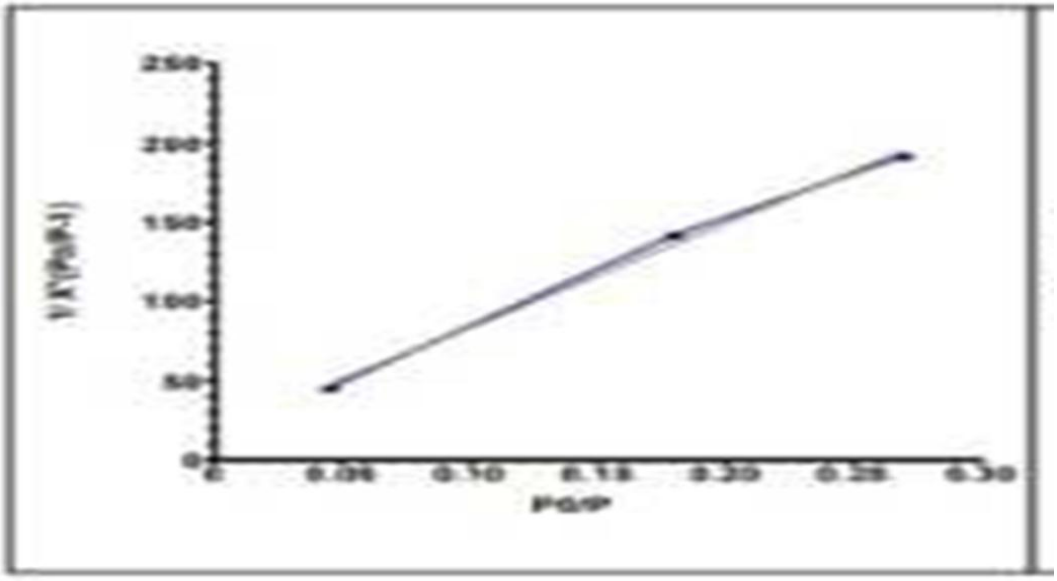

Figure 4.5b. N_2 adsorption-desorption isotherms of the synthetic zeolite.

Table 4.1: Surface characteristics of the kaolin, meta-kaolin and synthetic zeolite

Samples	**S_{BET} ($m^2 \cdot gm^{-1}$)**
kaolin	30.878
Meta-kaolinite	3.340
Zeolite-X	57.94

4.1.4. FTIR Results Analysis

The FTIR spectra were used for qualitative characterization of surface functional groups of the kaolin, Meta kaolin, and zeolite-X. As Figure 4.7a shows Kaolin indicates that the broad band observed at 1289 cm^{-1} was assigned as the Si-O in the molecule of SiO_4. The other vibration band was seen at 1412 cm^{-1} attributed to the Al-OH group. The bands recorded 640- 843cm^{-1} were symmetrical stretching of Si-O. The band for absorption value at 992.92 cm^{-1} was assigned for Si-O-Al, in which the Al^{3+} was found in octahedral coordination (Aragaw and Ayalew 2019).

Figure 4.7b showed that the conversion of kaolin to Meta-kaolin was the cause of the loss of these bands at 3300-3650 cm-1 associated with the OH functional group. These modifications were comparable to those noted in earlier research (Aragaw and Kuraz 2019). Three broad bands with centers at 943.04, 666.26, and 413.73 cm^{-1} were the distinctive bands in meta-kaolin. Amorphous SiO2 attributed to a considerable shift of the Si-O vibration bands at 1143 and 1324 cm^{-1} kaolin to a higher frequency band at 1143 cm^{-1} in meta-kaolin. Al- O-Si were in octahedra kaolin and found to stretch at a frequency of 520 cm^{-1}(Kwakye et al. 2022). A peak at 993 cm^{-1} that corresponded to the vibration band of the Al_2O_3 tetrahedron in meta-kaolin. These peaks represent the formation of the disordered phase of meta-kaolin(Kwakye et al. 2022).

Zeolite-x bands were observed in the FTIR spectra Fig 4.7c. The bands in the region of 413.73–519 cm-1 were attributed to inner tetrahedron vibrations of Si-O and Al-O or (T-O bands) of zeolite-X materials. The double ring vibrational bands occurred at 517-807.506 cm-1 indicating the (Al-O-Al) and (Si-O-Si) symmetric stretching of aluminates and silicates. Sharp and small dips at 964.44 cm-1 of FUZ demonstrate (Al-O-Al) and (Si-O-Si) symmetric stretching vibrations in synthesized zeolite-X. The peaks at 1302.42 cm-1 were assigned to external symmetric and internal asymmetric stretching of T-O-T (T=Si, Al) and Al atom present in tetrahedral. The band at 3337.11-3656.60 cm-1 indicates the presence of water, and it was a characteristic vibration band associated with stretching of the -O-H functional group, indicating the presence of bonded -O-H group or adsorbed water molecules in the sample. The presence of adsorbed water molecules was supported by the absorption band located at 1613.54 cm-1, commonly assigned to the bending vibration of adsorbed water molecules in the OH group (Aragaw and Ayalew 2019).

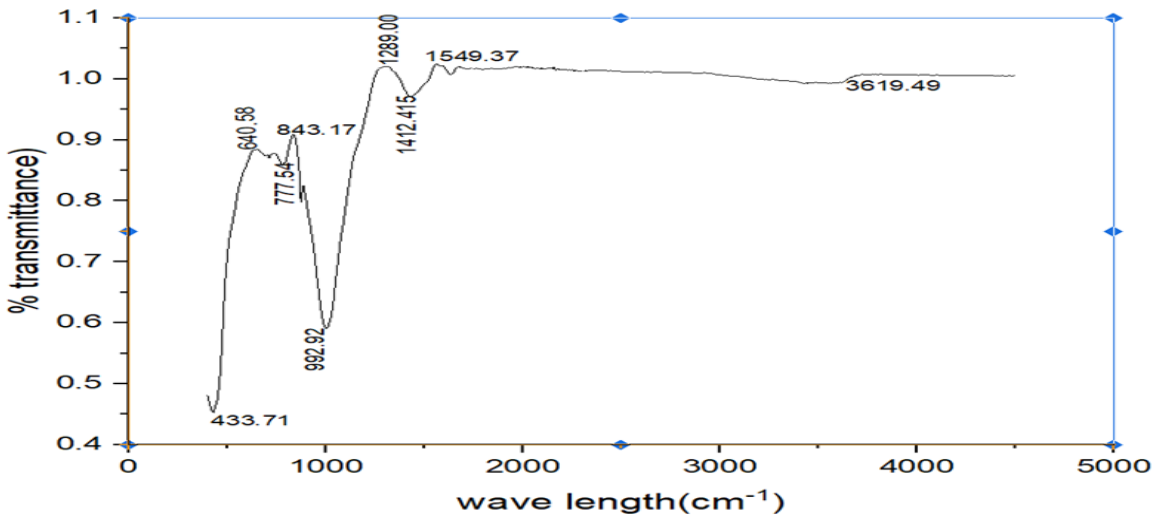

a. Kaolin

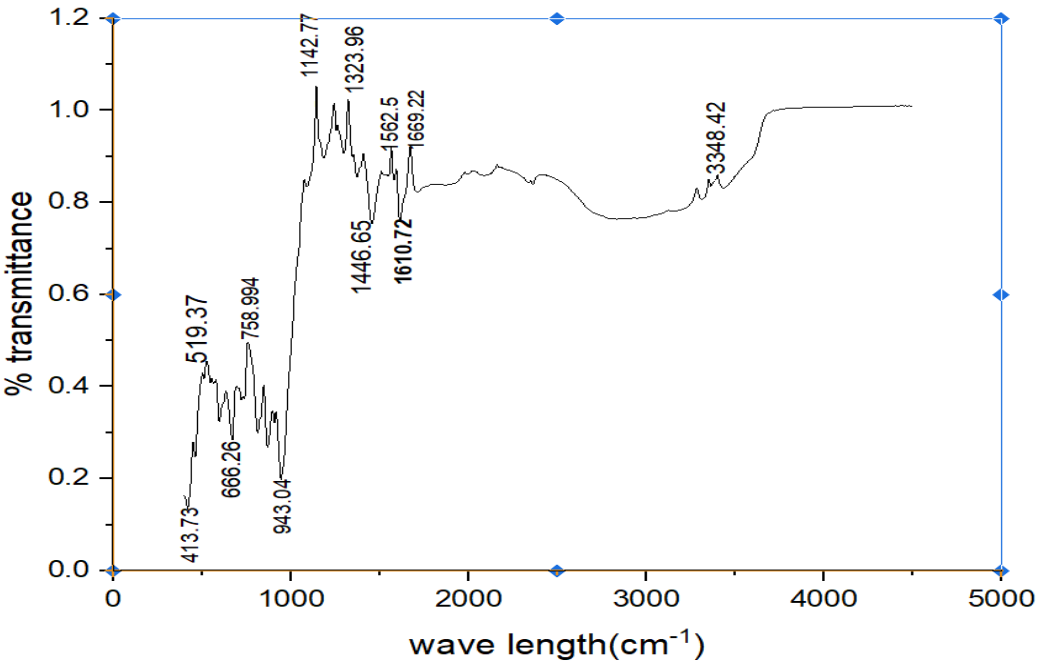

b. Meta-kaolinite

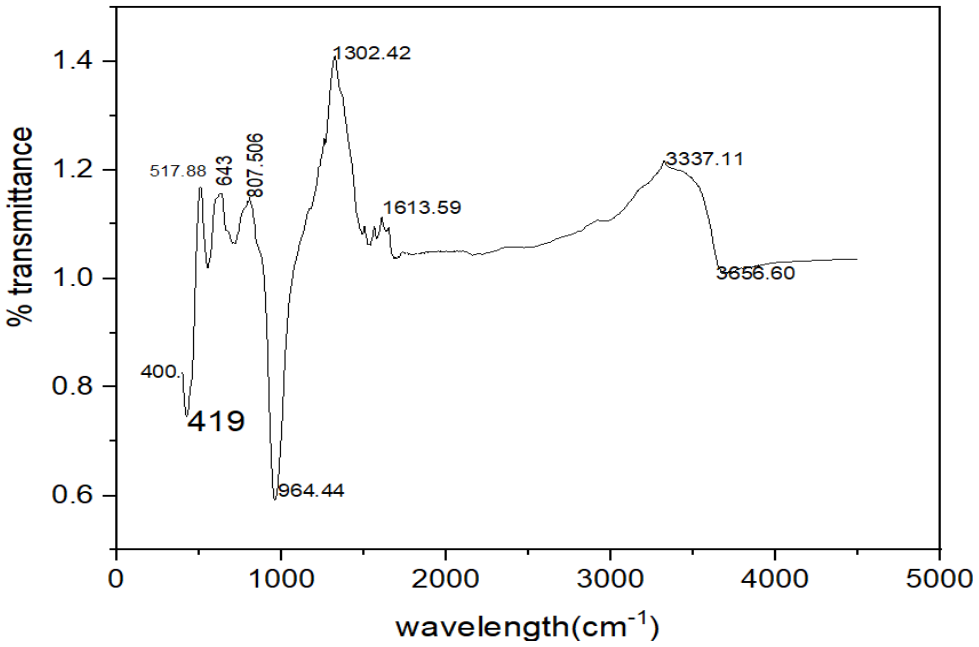

c. Zeolite-X

Figure 4. 6. FTIR Spectra of meta-kaolinite, kaolinite, synthesized zeolite-X, and synthesized zeolite with kaolinite and meta-kaolinite

4.2. Determination of Standard Calibration Curve for the Lead (II) in Aqueous Solution

The main analytical parameters listed in Table 4.2 were used to normalize the Pb (II) ion concentration. The detection limits (LOD = YB + 3SB) and quantification limits (LOQ = YB + 10SB), where YB is the blank signal and SB is the standard deviations of the regent blank, "b" is the gradient of the calibration curve, and an acceptable correlation (R2= 0.95670) were discovered in the linear range studied. The aggregated standard deviation of lead ions in the prescribed calibration range is 0.37632 mg/L for the application. The concentration of lead ion solution and absorbance have a positive association according to the statistical test at p = 0.04, and the average standard deviation of lead ion is 0.00172.

Table 4.2. Calibration curve for the standardization of the Pb(II) ion concentration

line	unit	conc	DF	Abs	SD	RSD	DATE	TIME	NAME	ABS	single value (Abs)	
Pb283	mg/L		0	0			5/19/2022	9:45				
Pb283	mg/L	0	1	0.00024	0.00007	28.9	5/19/2022	9:45	Cal-Zero1	0.00029	0.00028	0.00016
Pb283	mg/L	1	1	0.00053	0.00005	9.1	5/19/2022	9:46	Cal-Std1	0.00058	0.00049	0.00051
Pb283	mg/L	5	1	0.0024	0.00014	6	5/19/2022	9:47	Cal-Std2	0.00225	0.00241	0.00254
Pb283	mg/L	1	1	0.0004	0.00023	57.7	5/19/2022	9:49	Cal-Std1	0.00036	0.00019	0.00064
Pb283	mg/L	1	1	0.01205	0.00023	1.9	5/19/2022	9:54	Cal-Std1	0.01221	0.01216	0.01179
Pb283	mg/L	5	1	0.05435	0.00056	1	5/19/2022	9:55	Cal-Std2	0.05499	0.05398	0.05408
Pb283	mg/L	10	1	0.10229	0.0063	6.2	5/19/2022	9:55	Cal-Std3	0.0955	0.10345	0.10793
Pb283	mg/L	15	1	0.1459	0.00368	2.5	5/19/2022	9:56	Cal-Std4	0.14167	0.14765	0.14837
Pb283	mg/L	20	1	0.24865	0.00423	1.7	5/19/2022	9:57	Cal-Std5	0.24412	0.24934	0.25249
Pb283			0				5/19/2022	9:57				

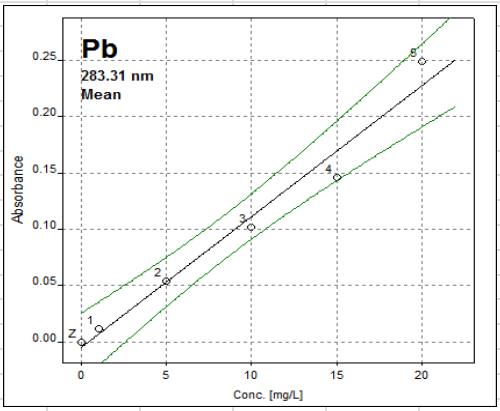

R^2(adj.): 0.95670 Slope:0.01 Char.conc.:0.37632 mg/L/1%A

4.3. Statistical Analysis of the Experimental Result

Table 4.3 shown that the operational variables i. e contact time, concentration of adsorbent ,concentration of lead (II)ion and pH using BOX-Behnken design(BBD) approach coupled with response surface method (RSM).

Table 4.3: Experimental design and results

	Factor 1	Factor 2	Factor 3	Factor 4	Response 1
Std	A:CONTACT TIME	B:mass of adsorbent	C:CONC,OF Pb	D:pH	removal of Pb(II) efficiency
	MIN	g	mg /L		%
1	15	0.5	15.5	6	95.09
2	90	0.5	15.5	6	97
3	15	5	15.5	6	96.03
4	90	5	15.5	6	96.02
5	52.5	2.75	1	3	97.05
6	52.5	2.75	30	3	85.4
7	52.5	2.75	1	9	96
8	52.5	2.75	30	9	87
9	15	2.75	15.5	3	93.5
10	90	2.75	15.5	3	96.27
11	15	2.75	15.5	9	93.5
12	90	2.75	15.5	9	96.39
13	52.5	0.5	1	6	98.2
14	52.5	5	1	6	97
15	52.5	0.5	30	6	86.05
16	52.5	5	30	6	89.012
17	15	2.75	1	6	96
18	90	2.75	1	6	98.19
19	15	2.75	30	6	85.3
20	90	2.75	30	6	86.04
21	52.5	0.5	15.5	3	96.9
22	52.5	5	15.5	3	96.04
23	52.5	0.5	15.5	9	96
24	52.5	5	15.5	9	96.27
25	52.5	2.75	15.5	6	97.29
26	52.5	2.75	15.5	6	97.97
27	52.5	2.75	15.5	6	97.27
28	52.5	2.75	15.5	6	97.97
29	52.5	2.75	15.5	6	97.97

Table 4.4: Analysis of Variance (ANOVA) of the Response of Removal of Lead (II) Ion Efficiency

Source	Sum of Squares	df	Mean Square	F-value	p-value	
Model	521.76	14	37.27	115.10	< 0.0001	significant
A-CONTACT TIME	9.17	1	9.17	28.32	0.0001	
B-mass of adsorbent	0.1068	1	0.1068	0.3298	0.5749	
C-CONC,OF Pb	337.48	1	337.48	1042.29	< 0.0001	
D-pH	0.0000	1	0.0000	0.0000	1.0000	
AB	0.9216	1	0.9216	2.85	0.1137	
AC	0.5256	1	0.5256	1.62	0.2234	
AD	0.0036	1	0.0036	0.0111	0.9175	
BC	4.33	1	4.33	13.37	0.0026	
BD	0.3192	1	0.3192	0.9859	0.3376	
CD	1.76	1	1.76	5.42	0.0354	
A^2	13.47	1	13.47	41.61	< 0.0001	
B^2	0.1579	1	0.1579	0.4875	0.4965	
C^2	159.08	1	159.08	491.31	< 0.0001	
D^2	11.26	1	11.26	34.77	< 0.0001	
Residual	4.53	14	0.3238			
Lack of Fit	3.96	10	0.3962	2.77	0.1689	not significant
Pure Error	0.5715	4	0.1429			
Cor Total	526.29	28				

Factor coding is **coded**. Sum of squares is **Type III - Partial**

The **Model F-value** of 115.10 implies the model is significant. There is only a 0.01% chance that an F-value this large could occur due to noise.

P-values less than 0.0500 indicate model terms are significant. In this case A, C, BC, CD, A^2, C^2, D^2 are significant model terms While the terms B, D, AB, AC, AD, BD, B^2 were not significant . If there are many insignificant model terms (not counting those required to support hierarchy), model reduction was improved your model.

The **Lack of Fit F-value** of 2.77 implies the Lack of Fit is not significant relative to the pure error. There is a 16.89% chance that a Lack of Fit F-value this large could occur due to noise. Non-significant lack of fit is good -- we want the model to fit.

Table 4.5: Predicted and adjusted value of removal efficiency of lead (II) ion

Std. Dev.	0.5690	**R^2**	0.9914
Mean	94.44	**Adjusted R^2**	0.9828
C.V. %	0.6025	**Predicted R^2**	0.9549
		Adeq Precision	32.6862

The **Predicted R^2** of 0.9549 is in reasonable agreement with the **Adjusted R^2** of 0.9828; i.e. the difference is less than 0.2.

Adeq Precision measures the signal to noise ratio. A ratio greater than 4 is desirable. Your ratio of 32.686 indicates an adequate signal. This model can be used to navigate the design space.

Final Equation in Terms of Coded Factors

(Removal efficiency of lead (II) ion)Y = 97.694 + 0.874167 * A + 0.0943333 * B + -5.30317 * C + -8.55845e-16 * D + -0.48 * AB + -0.3625 * AC + 0.03 * AD + 1.0405 * BC + 0.2825 * BD + 0.6625 * CD + -1.44125 * A^2 + -0.156 * B^2 + -4.95225 * C^2 + -1.3175 * D^2

The equation in terms of coded factors can be used to make predictions about the response for given levels of each factor. By default, the high levels of the factors are coded as +1 and the low

levels are coded as -1. The coded equation is useful for identifying the relative impact of the factors by comparing the factor coefficients.

Final Equation in Terms of Actual Factors

(Removal efficiency of lead (II) ion)Y = 90.2235 + 0.155302 * A + -0.235374 * B + 0.220357 * C + 1.39151 * D + -0.00568889 * AB + -0.000666667 * AC + 0.000266667 * AD + 0.0318927 * BC + 0.0418519 * BD + 0.0152299 * CD + -0.00102489 * A^2 + -0.0308148 * B^2 + -0.0235541 * C^2 + -0.146389 * D^2

The equation in terms of actual factors can be used to make predictions about the response for given levels of each factor. Here, the levels should be specified in the original units for each factor. This equation should not be used to determine the relative impact of each factor because the coefficients are scaled to accommodate the units of each factor and the intercept is not at the center of the design space.

Where: A: contact time, B: concentration of adsorbent, C: concentration of lead (II) ion and D: pH

4.3.1. Interaction Effects of Process Variables on Pb (II) ion Removal

Using contour and 3D plots of three dimensional views of the response surface as a function of two independent factors, preserving all other variables at a fixed or varying level, the interaction impact of process variables for % removal of Pb (II) ion using zeolite-X was displayed. Understanding the direct and indirect impacts of the independent variables on the response variable using these charts was beneficial.

4.3.1.1. The Interaction Effect of mass of Adsorbent Dosage and Concentration of Lead (II) Ion (BC)

From the interaction graph observed that as the initial concentration increase and the adsorbent dose increase the removal efficiency also increase. The interaction of both factors lead (II) concentration and adsorbent dose can be analyzed by the 3D plot of Fig 4.7. The increased initial concentration of lead (II) with an increase in the adsorbent dose of zeolite might be due to the availability of more surface area with more functional groups at the higher mass of adsorbent (Chai et al., 2020)

The interaction effect between the mass of adsorbent dosage and the concentration of lead (II) ion (BC) can significantly impact the adsorption process. Adsorbents are materials used to remove lead (II) ion from a solution, and in this case, we are considering their effectiveness in removing lead (II) ions. The mass of adsorbent dosage refers to the amount of adsorbent material added to the system. Increasing the mass of adsorbent dosage can potentially enhance the adsorption capacity and efficiency of the process. With a higher mass of adsorbent, there is a larger surface area available for adsorption, allowing for more lead (II) ions to be captured and removed from the solution. However, it is important to find the optimal mass of adsorbent dosage to achieve the best results. Too little adsorbent may result in incomplete removal, while too much adsorbent can lead to inefficient utilization and increased costs. The amount of lead (II) ions present in the solution, represented by BC, is another critical factor. Higher initial concentrations of lead (II) ions can provide a greater driving force for adsorption. As the concentration increases, more lead (II) ions will come into contact with the adsorbent, increasing the chances of successful adsorption. However, at very high concentrations, the adsorbent's adsorption capacity may become saturated, resulting in lower removal efficiency. To understand the interaction effect between the mass of adsorbent dosage and the concentration of lead (II) ions, it is basic to conduct experiments with varying levels of both variables. By measuring the adsorption capacity, removal efficiency, and equilibrium concentration of lead (II) ions, we can determine the optimal conditions for effective adsorption(Chai et al. 2020).

Studying the interaction effect between the mass of adsorbent dosage and the concentration of lead (II) ions is crucial for optimizing the adsorption process. This knowledge can contribute to the development of efficient and cost-effective methods for removing lead (II) ions from contaminated water sources in Ethiopia, ensuring the provision of clean and safe water for the population.

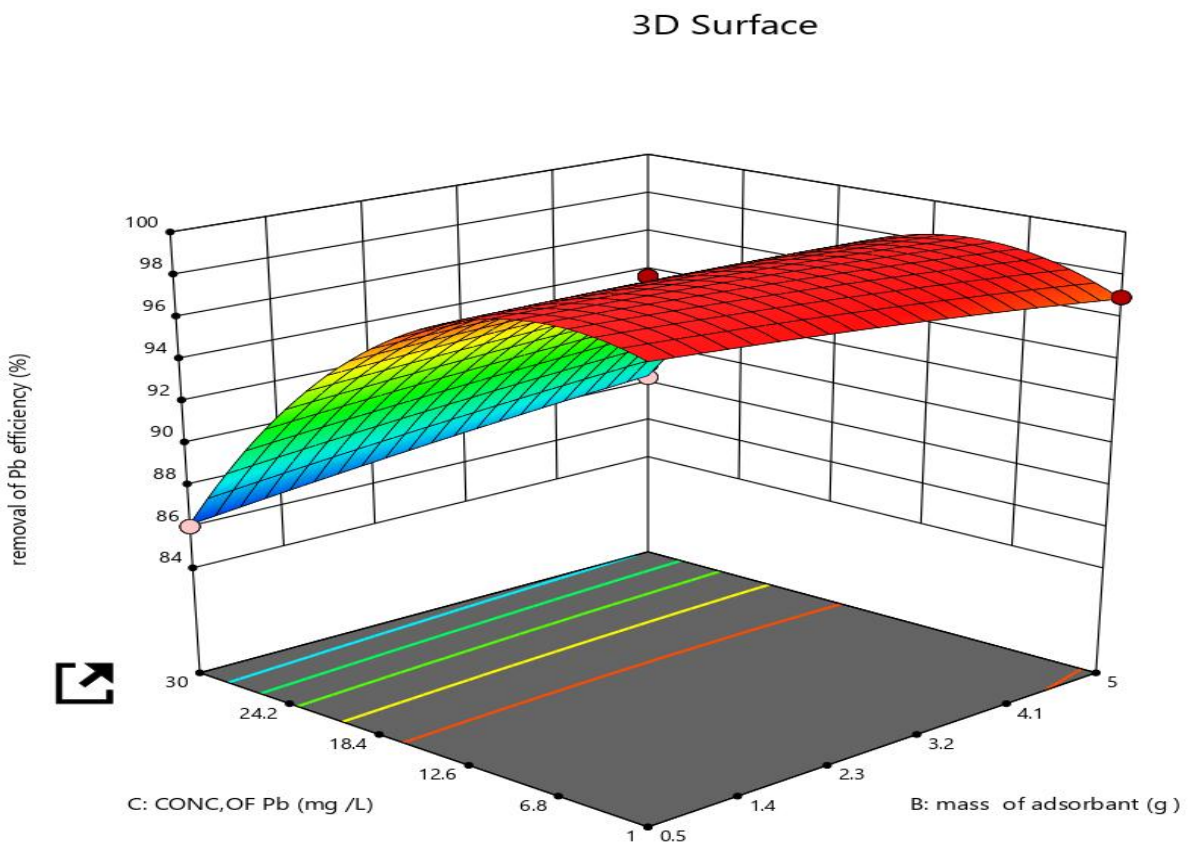

Figure 4. 7.3D plot of lead (II) ion removal showing the interaction effect of Initial metal ions concentration and concentration of adsorbent dosage

4.3.1.2 The Interaction Effect of Concentration of Pb (II) Ion and Concentration of pH (CD)

Figure 4.6 shows that at their mid-level values, both pH and starting metal ion concentration have a considerable influence on lead (II) ion removal. Lower level values of both components and subsequent escalation beyond mid values demonstrated a reduction in lead (II) ions removal efficiency. The plot shows that the most lead was removed at pH=6, with an initial concentration of 15.5mg/L, a fixed adsorbent dosage of 2.75g, and a contact duration of 52.5 minutes. As a result, when the pH of the medium increases, so does cation adsorption, since negatively charged adsorbent surfaces bind firmly and promptly to lead(II) ions beyond the adsorbent site's mid-value limit. In addition, the interaction effect between the concentration of Pb (II) ions and the concentration of pH (CD) can have a significant impact on various processes involving lead (II) ions, such as adsorption, precipitation, or complexation. The concentration of Pb (II) ions refers to the amount of lead ions present in a solution. Higher concentrations of Pb (II) ions can lead to

increased interactions with other compounds or surfaces. This can enhance the likelihood of adsorption onto solid surfaces or the formation of precipitates or complexes. However, excessively high concentrations of Pb (II) ions can also lead to saturation or hinder the desired reactions. The concentration of pH, on the other hand, represents the level of acidity or alkalinity in a solution. pH plays a crucial role in determining the speciation and reactivity of Pb (II) ions. Different pH conditions can influence the solubility and complexion behavior of lead ions. For example, at low pH values (acidic conditions), Pb (II) ions tend to exist as free ions or form simple complexes. In contrast, at higher pH values (alkaline conditions), lead ions may form hydroxide precipitates or complex with other ligands(Weyrich et al. 2023).

The interaction effect between the concentration of Pb (II) ions and the concentration of pH can be studied by conducting experiments with varying levels of both variables. By measuring the changes in speciation, solubility, or reactivity of lead (II) ions under different pH conditions and concentrations, we can understand the interplay between these factors and optimize processes such as adsorption or precipitation. Understanding the interaction effect between the concentration of Pb (II) ions and the concentration of pH is crucial, especially in environmental and analytical chemistry. This knowledge can help in designing effective strategies for the removal or recovery of lead (II) ions from contaminated water sources, soil, or industrial effluents. Additionally, it can help determine appropriate pH conditions for safe disposal or processing of lead-containing waste (Lin, Li, & Cheng, 2016).

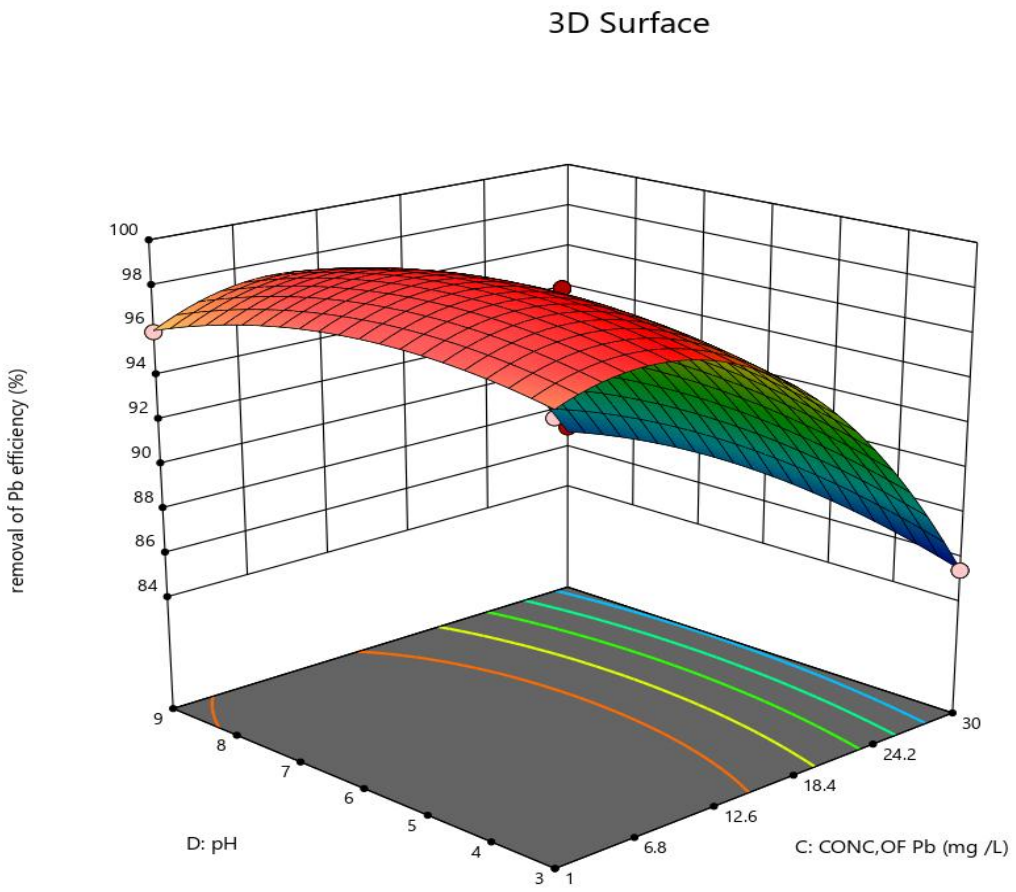

Figure 4.8:3D plot of lead (II) ion removal showing the interaction effect of Initial metal ions concentration and pH

4.3.2. Diagnostics Plot

One way to determine whether a data set was roughly normally distributed is to look at the normal plot of the residuals graph for Fig. 4.9a. The straight line means that no response transformation was required and that there was no apparent problem with normality. The experimental results were compared to a theoretical normal distribution such that the points should roughly form a straight line. By looking at the plots of anticipated vs. experimental % yield and elimination, as illustrated in Fig. 4.7 b and c, one can also see how well the model performs. The anticipated values for lead (II) ion adsorption were the ones that were most similar to their experimental values

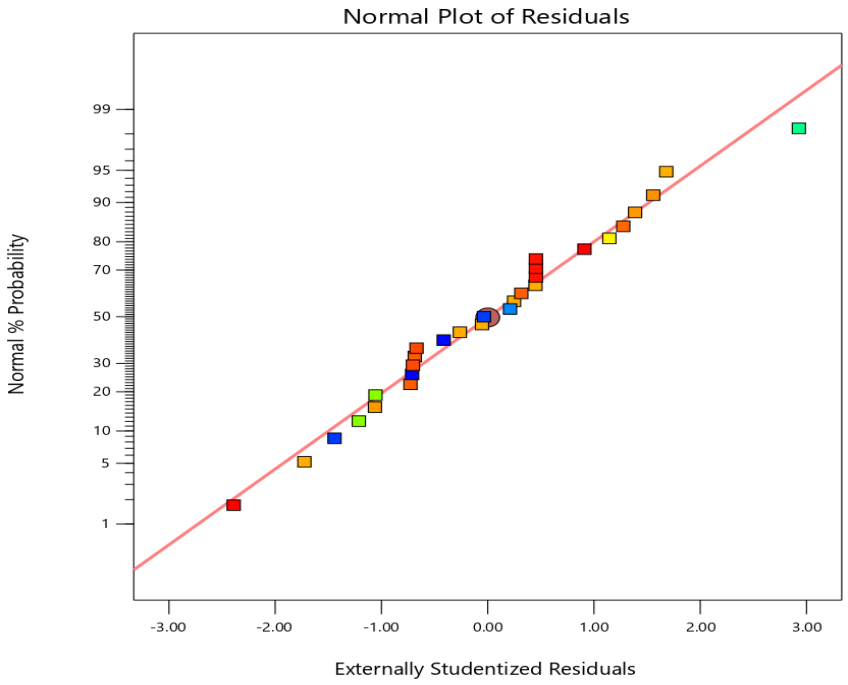

Figure 4.9a. Normal plot of residuals experimental value for removal efficiency of lead by zeolite-X

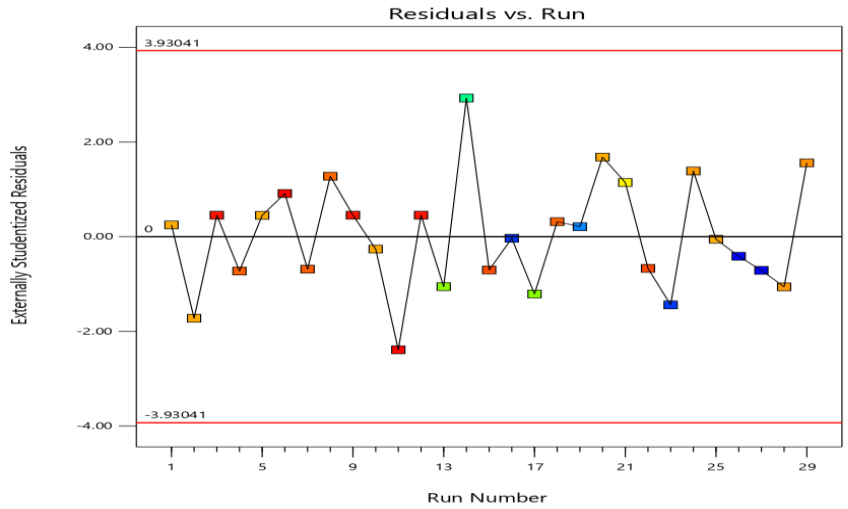

Figure 4.9b. Residual vs experimental

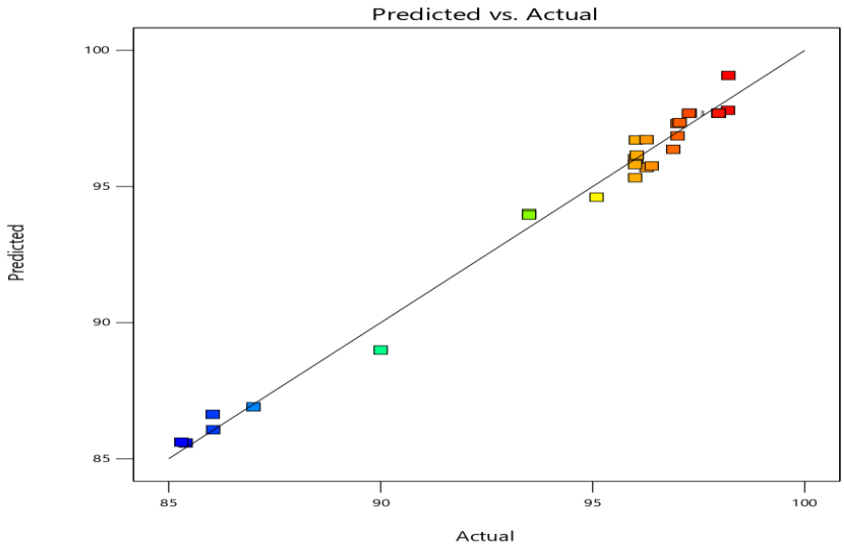

Figure 4.9c. Predicted vs actual value for removal efficiency of lead (II) by zeolite

4.4. Adsorption Studies Using Different Parameters

4.4.1. Effect of pH of the Solution on Adsorption of Pb (II) ion

The effects of pH on a solution were a major factor used to determine the adsorption property of an adsorbent from wastewater. In this study, the effects of pH were tested by changing the pH of the solution in the range of 3, 6, and 9.

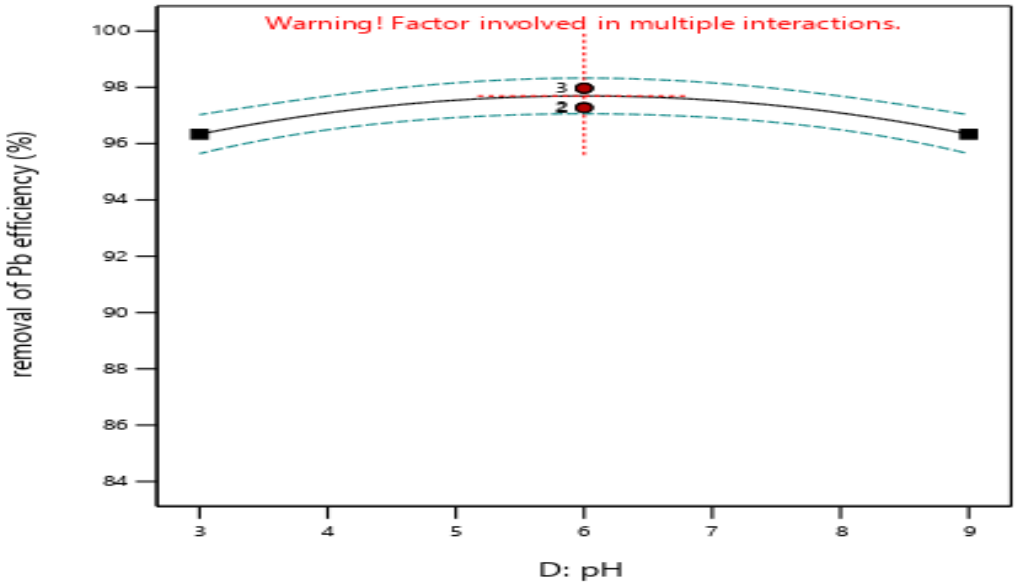

Figure 4. 10. Effects of pH on the removal efficiency

In Fig. 4.10 the percentage removal of Pb (II) ions increased from 95.9% to 97.27%. When the pH of the solution was correspondingly increased from 3 to 6 and decreased from 6 to 9. Previous research has shown that increasing the pH of the medium enhances negatively charged Pb (II) compounds compared to positively charged compounds, and that the pH of the solution should be near 6-8 for efficient metal ion sequestration. A solution with a pH $\leq$ 4 has significant concentrations of H^+ ions, which interfere with soluble metal cations and adsorbent surface sites, resulting in competition for attachment and a reduction in metal removal from wastewater(Abdel-magid 2015) . However, as the pH of the medium rises, cation adsorption rises as well, because negatively charged adsorbent surfaces adhere firmly and immediately to hazardous metal cations(Ariana 2016)(Hussain et al. 2021). Precipitation is the dominant phenomenon at higher pH (>=10) due to the development of insoluble hydroxides of respective metals, in this case, $Pb(OH)^2$ and soluble hydroxyl complexes such as $Pb(OH)^+$, aqueous $Pb(OH)_2$, and $Pb(OH)^{3-}$. (2015) Kabwadza-Corner, Johan, and Matsue

In general, the adsorption of Pb (II) ions onto adsorbent surfaces is favored under acidic to neutral pH conditions. At lower pH values, the adsorbent surface tends to have a net positive charge. This electrostatic attraction between the positively charged surface and the Pb (II) ions facilitates their adsorption. Additionally, the Pb (II) ions themselves remain in their ionic form under acidic conditions, making them more accessible for adsorption.

However, as the pH value of the solution increases and becomes more alkaline, the adsorption of Pb (II) ions tends to decrease. This is because the adsorbent surface may become negatively charged, resulting in electrostatic repulsion with the Pb (II) ions. Furthermore, under alkaline conditions, the Pb (II) ions can form hydroxide complexes, making them less available for adsorption onto the surface. It is critical to consider the pH of the solution while optimizing the adsorption of Pb (II) ions. Experiments with changing pH levels can aid in determining the pH range at which adsorption effectiveness is maximized. This knowledge is critical for developing effective adsorption techniques for removing Pb (II) ions from polluted water sources or industrial effluents. Finally, the pH of the solution has an impact on the adsorption of Pb (II) ions. Understanding this connection is critical for creating effective and dependable strategies for removing Pb (II) ions from a variety of environmental and industrial sources(Samadi et al. 2019)

4.4.2. Effects of Adsorbent on the Removal of Pb (II)

The adsorbent dosage is an important parameter in the adsorption studies because it determines the capacity of the adsorbent for a given initial concentration of Pb (II) solution. For this study, the effect of dosage was investigated by changing the adsorbent in the range 0.5, 2.75, and 5 g and at a constant initial concentration Pb (II) of 15.5 mg/L and constant pH of 6. The result from Figure 4.8 showed that the removal of Pb (II) increased from 97.32 % to 97.39% with increasing adsorbent dose from 0.5 to 5 g respectively. This is because for a fixed initial metal concentration while increasing the adsorbent dose provides a greater adsorption site, but at 2.75 g there is a small decrement to 97.27% with an unknown reason.

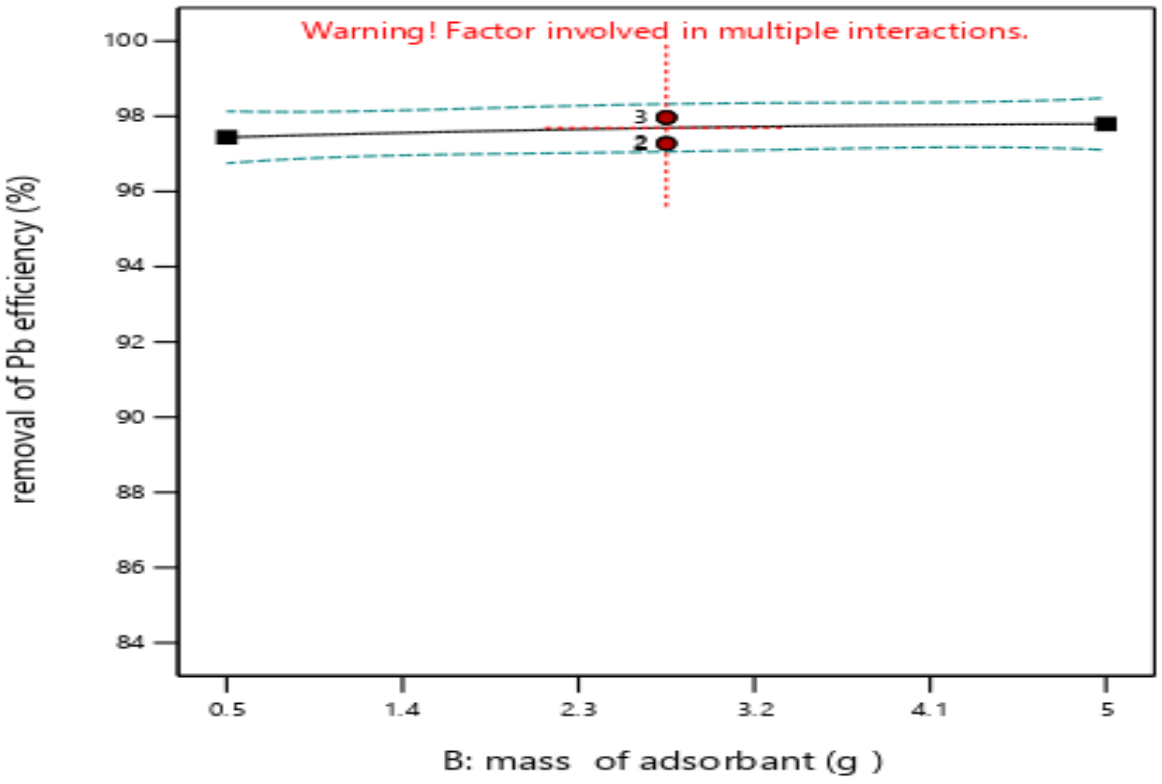

Figure 4. 11: Effect of Adsorbent Dose on Removal Efficiency

This result can be described as the fact that some of the adsorption sites remain unsaturated after the adsorption process. Even if the up-take of the metal increased by increasing the adsorbent dose, beyond a dose of 2.75 g and less than it even and the rise of the adsorption efficiency was insignificant and the capacity of adsorbent was very low. Therefore 2.75 g of adsorbent was

taken as an optimum dose for further experiment. Similar results were reported (Udeh, N.U, Agunwamba, 2017) in the removal of Pb (II) from aqueous solution using other adsorbents.

4.4.3. Effects of Initial Concentration on the Removal of Pb (II) ion

Better removal was achieved at the initial Pb (II) ion concentration of 15.5 mg/L (Fig. 4.10). The removal of Pb (II) ion was decreased with the increased concentration from 1 to 30 mg/L; because of the low concentration, there was a low number of lead ions to the ratio of the surface-active site found in the adsorbent surface. Therefore, all of the lead ions may interact with the active site. In contrast, when a higher initial concentration proved more lead ions for being attached to the adsorbent surface. More exchangeable sites are available at the Na-zeolite surface than sorbate ions, which is what drives the process. The active sites on the adsorbent surface become saturated, however, at very high initial lead (II) ion concentrations, making these adsorbents (Na-zeolites) unable to effectively remove the metal ions from wastewater (Hussain et al., 2021b). The result, the active site was not sufficient and unchanged hence saturation in the adsorbent happened it resulting in the reduction of removal efficiency (Panek et al., 2021).

In Addition, the initial concentration of Pb (II) ions in a solution has a notable effect on the removal efficiency of these ions. As the initial concentration increases, several factors come into play, influencing the removal process. Firstly, a higher initial concentration of Pb (II) ions provides a greater driving force for adsorption or other removal mechanisms. With more Pb (II) ions present in the solution, there is a larger concentration gradient between the solution and the adsorbent surface. This gradient enhances the mass transfer of Pb (II) ions onto the adsorbent, resulting in higher removal efficiency(Alboghbeish, Larki, and Saghanezhad 2022).

Fortunately, if the initial concentration of Pb (II) ions grows, the adsorbent's adsorption ability may become restricted. Adsorbents have a finite capacity to adsorb ions, and at increasing concentrations, the adsorbent surface's accessible adsorption sites may become saturated. As the adsorbent approaches its maximum adsorption capacity, this might result in decreased removal effectiveness. Furthermore, complexes or precipitates can develop at exceedingly high starting concentrations. These complexes or precipitates may obstruct adsorption or result in the production of bigger particulate debris that is more difficult to remove. It is critical to consider the beginning concentration while optimizing the removal of Pb (II) ions. Experiments with

varied beginning concentrations can assist in determining the range within which the removal efficiency is maximized. This information is valuable in designing effective treatment processes for the removal of Pb (II) ions from contaminated water sources or industrial effluents (Weyrich et al. 2023).

In summary, the initial concentration of Pb (II) ions significantly affects their removal efficiency. While higher initial concentrations provide a greater driving force for removal, there is a limit to the adsorption capacity of the adsorbent. Understanding this relationship is vital for developing efficient and reliable methods for the removal of Pb (II) ions from different sources.

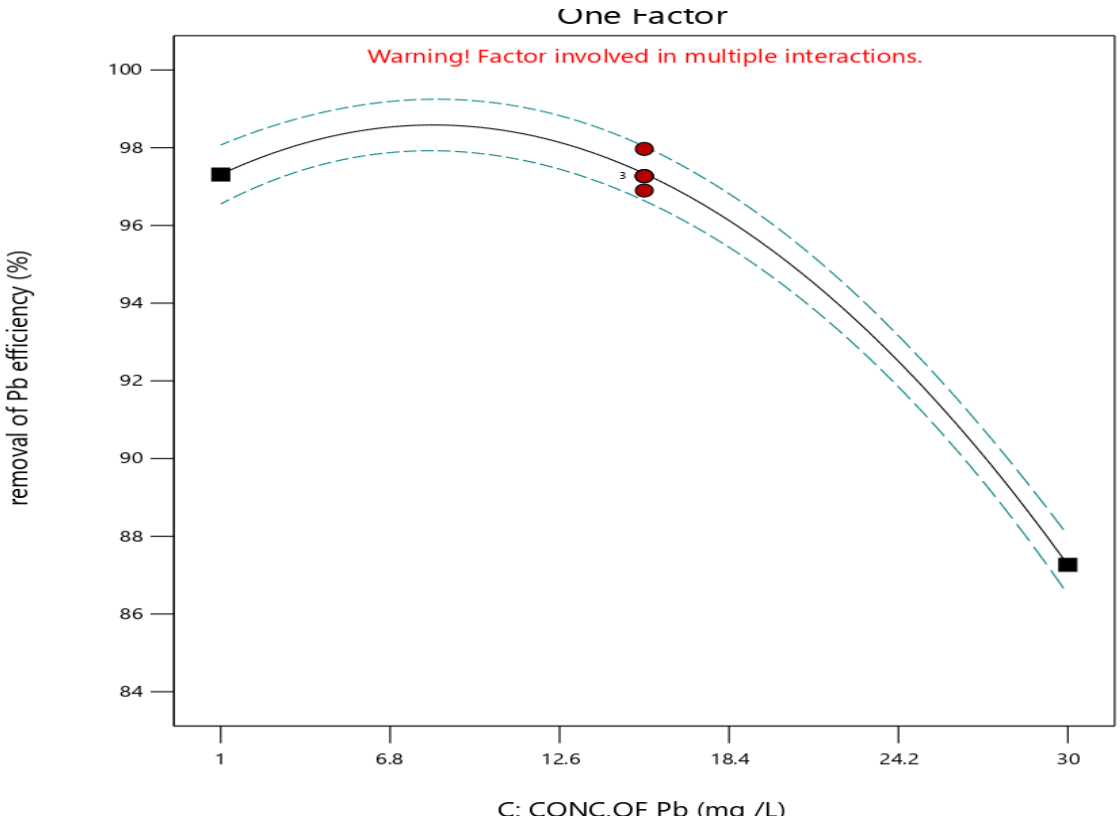

Figure 4.12: Effects of Initial Concentration on removal efficiency

4.4.4. Effect of Contact Time on Removal of Lead

Figure 4.12 shows the effect of contact time on the adsorption of lead ions by the produced zeolite Na-X at an initial concentration of Pb (II) ions of 15.5 mg/L, an adsorbent dose of 2.75 g,

and a pH of 6. At the outset of the sorption process, an extensive number of active locations are accessible on adsorbent surfaces, and a significant quantity of metal ions boosts the rate of sorption. After 52.5 minutes of absorbency, the absorbent areas of the Na-zeolite surface diminish and the Pb (II) ions reach a lower quantity, rendering them unable to boost the adsorbent's removal effectiveness. The contact time during the sorption of Pb (II) removal from wastewater shows rapid adsorption initially, and, thereafter, it decreases gradually or remains constant to achieve equilibrium in a shorter period of time, about 52.5 min. A further increase in contact time has an inverse and non-significant effect on removal efficiency (Bayuo, Rwiza, and Mtei, 2022b)

The synthesized Na-zeolite adsorbents get saturated, they restrict the further diffusion of Pb (II), which reduces the significance of prolonged contact times. The plots reveal that maximum percentage removal was highest during the first 52.5 min of adsorption, as a large surface area and active adsorbent sites were available. At the starting stage of adsorption, the rate of Pb (II) uptake is due to the transportation of charged species into the interior of the cage structure of Na-zeolites. More than 97.27 % of the total adsorption occurred within the first 52.5 min and after 52.5 min, the lead ions adsorption by the zeolite NaX did not significantly change with time. For more explanation

The effect of contact time on the adsorption of lead ions by zeolite can be summarized as follows: Initial Rapid Adsorption: At the beginning of the contact time, there is often a rapid adsorption of lead ions onto the zeolite surface. This occurs due to the availability of vacant adsorption sites on the zeolite, which readily attract and bind lead ions. During this stage, the lead ions quickly interact with the zeolite surface, resulting in a significant reduction in lead concentration. Equilibrium Phase: As the contact time progresses, the adsorption rate gradually decreases. This is because the zeolite's adsorption sites become occupied, requiring more time for additional lead ions to find available sites.

The system is approaching equilibrium, which occurs when the rate of adsorption equals the rate of desorption. This stage indicates that the zeolite has attained its maximal capacity for lead ion adsorption. Saturation Point: The adsorption process reaches a saturation point after a particular amount of contact time. At this point, the zeolite surface is completely coated with lead ions, and

additional contact time has no appreciable effect on lead ion removal. To optimize the adsorption process and establish the most efficient contact time for lead ion elimination, this point must be identified. In summary, the effect of contact time on the removal of lead ions through zeolite adsorption is characterized by an initial rapid adsorption phase, followed by a gradual decrease in adsorption rate until reaching equilibrium. Understanding the optimal contact time is crucial for maximizing the efficiency of lead ion removal using zeolite as an adsorbent. Similar results were found in other studies(Bayuo et al. 2018) therefore, the time of 52.5 min was selected as the equilibrium time for further experiments.

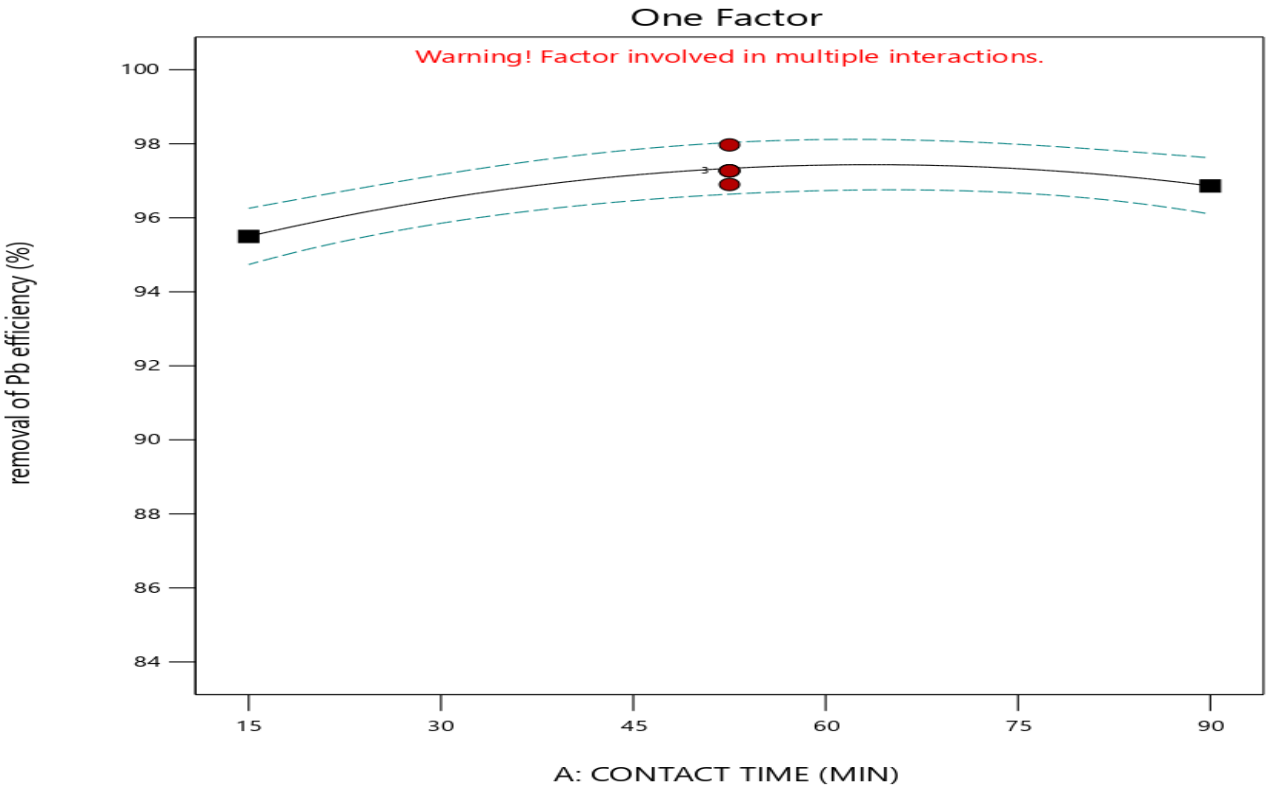

Figure 4.13: Effect of contact time on removal of Pb (II) Ion

4.5. Optimization

The study's goal was to enhance the efficiency of lead (II) ion removal from wastewater. The Response Surface Method, as shown in Table 4.6, may be used to determine the optimal combination of influencing factors for the removal efficiency of lead (II) ions from wastewater. The option with the highest attractiveness was picked from a selection of ideal solutions. As a result, in the current study, the intended aim for each element as well as the response

function were chosen. A target for initial lead (II) ion concentration in a range, contact duration in a range, adsorbent concentration in a range, and pH in a range with the maximum attractiveness was chosen. Design Expert 13.0.1 is a statistical software product.

Table 4.6: Criteria of setting factors to be optimized

Name	Goal	Lower Limit	Upper Limit	Lower Weight	Upper Weight	Importance
A:CONTACT TIME	is in range	15	90	1	1	3
B:mass of adsorbent	is in range	0.5	5	1	1	3
C:CONC,OF Pb	is in range	1	30	1	1	3
D:pH	is in range	3	9	1	1	3
removal of Pb efficiency	maximize	85.3	98.2	1	1	3

From the proposed numerical solutions provided below (in Table 4.7), it was observed that the optimum operating conditions for variables of the study were: 51.8 min of contact time, 4.5 g of concentration of adsorbent, 12.8mg/L initial concentration of lead (II) ion, 5.2 pH, and the predicted value of 98.2% of removal efficiency of lead (II) ion with its corresponding maximum desirability of 1.0

Table 4.7. Numerically optimized variables

Number	CONTACT TIME	Mass. of adsorbent	CONC,OF Pb	pH	removal of Pb efficiency	Desirability	
1	**51.793**	**4.506**	**12.785**	**5.179**	**98.200**	**1.000**	**Selected**

4.6. Adsorption Isotherm

To determine the kinetics of adsorption, batch equilibrium experiments were performed. A 100 ml conical flasks were used under optimal conditions of 12.8mg/L lead (II) ion, pH 5.2, 4.5 g zeolite-X adsorbent dose, and contact period (15, 30, 45, 60, 75, and 90 min). Langmuir and Freundlich isotherm models were used to calculate the maximal sorption capacity of zeolite-X.

Freundlich Isotherm and Langmuir Isotherm The slope and intercept of the plot of the quantity of sorbed lead (II) ions per unit mass, qt, versus the equilibrium concentration of metal ions remaining in solution, Ct, presented in Fig. 4.14, were used to calculate the correlation coefficient and constants of lead (II) ion zeolite-X sorption. The plot of (Ct) vs. Ct/qt revealed that the experimental data matched well in the linear equation of the Langmuir isotherm over the whole Lead (II) ion concentration range investigated. According to the values in Table 4.9, the maximum adsorption capacity of zeolite Na-X for Lead (II) ion was determined to be 39.67 mg/g. It should be noted that the surface of zeolite-X is homogenous, with Lead (II) ion adsorption forming a monolayer on its outer surface. In addition, the values of RL indicating favorable adsorption were calculated as shown in Table 4.8 and this showed that the process was favorable as its value was between 0 and 1.

Furthermore, linear plots of log qt vs. log Ct are shown in Fig. 4.15, proving that the Freundlich isotherm was also predictive of Lead (II) ion adsorption by zeolite-X (Na-X). Using a log qt vs. log Ce plot, the empirical constants KF and 1/n may be determined from the intercept and slope of the linear regression. In this work, the Langmuir isotherm has a better fitting model than Freundlich's, as the Langmuir model has a higher correlation regression coefficient than it, and demonstrates the applicability of Lead (II) ion monolayer coverage on the adsorbent's surface(Khayyun and Mseer 2019). The findings of the Langmuir and Freundlich models, as well as the fitted parameters, are shown in Table 4.9

Table 4.8: Experimental data of adsorption for Langmuir isomerism and Freundich isomerism

T(min)	Ci(mg/L)	Ct(mg/g)	qt(mg/g)	Ct/qt(g/L)	logCt	logqt
15	12.785	1.7035	0.306180648	5.563708912	0.231342138	-0.514022262
30	12.785	0.10179	0.341369285	0.345373779	-0.928486195	-0.466775557
45	12.785	0.0137	0.341684421	0.303496424	-0.984221244	-0.466374823
60	12.785	0.0235	0.34346427	0.068420509	-1.628932138	-0.464118435
75	12.785	0.0545	0.342776298	0.158995824	-1.263603498	-0.464989216
90	12.785	0.0545	0.342707501	0.168073356	-1.239577517	-0.46507639

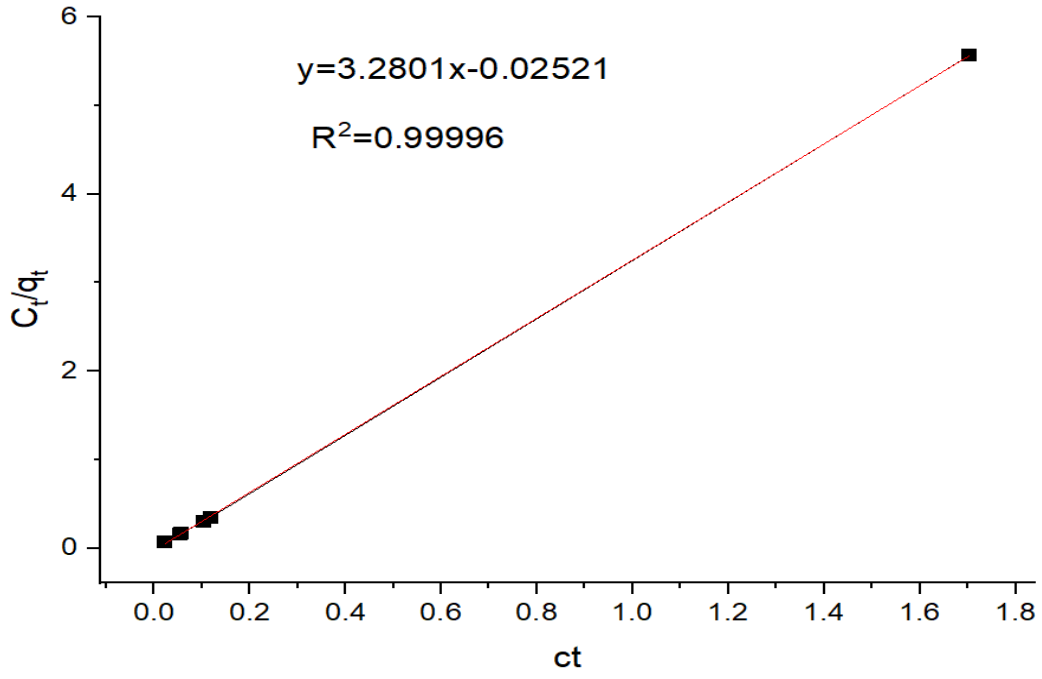

Figure 4. 14.Langmuir isotherm plot for adsorption of Lead (II) ion

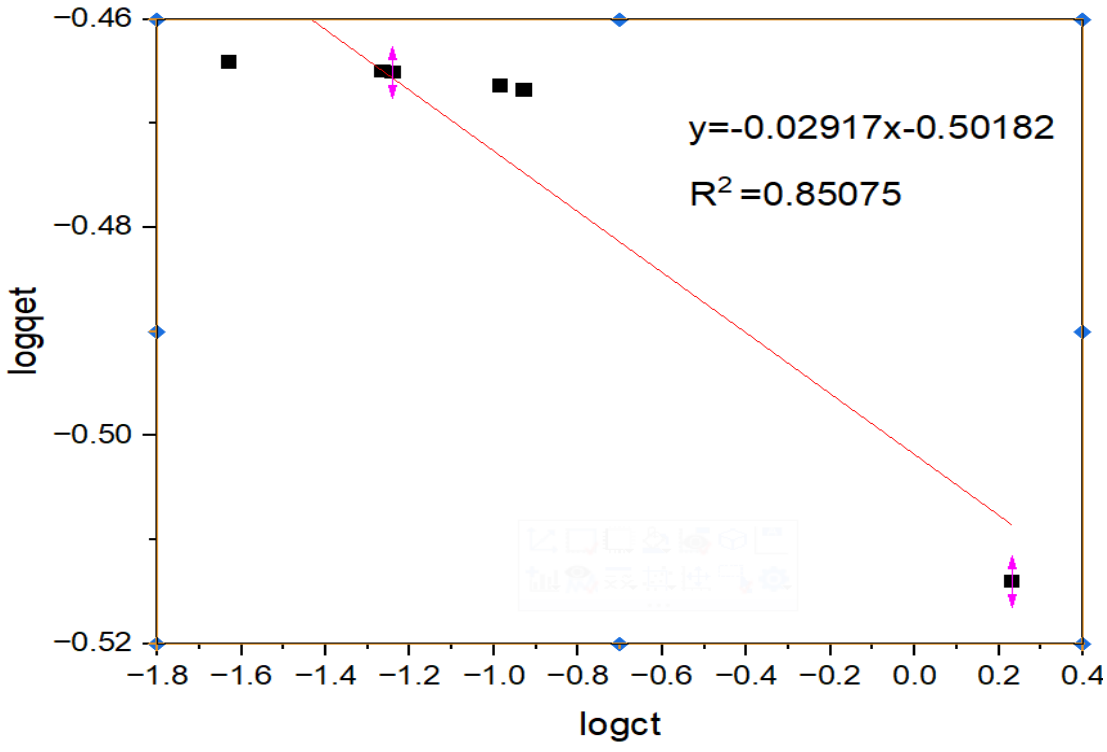

Figure 4.15. Freundlich isotherm plot for adsorption of Lead (II) ion

Table 4.9:Langmuir and Freundlich isotherm parameters for the adsorption of Lead (II) ion onto Na-X zeolite

	LANGMUIR PARAMETERS				FREUNDLICH PARAMETERS			
b(L/g)	**R_L**	**qm(mg/g)**	**K_L(L/mg)**	**R^2**	**Slope**	**1/n**	**Kf((mg/g)/(L/mg)1/n)**	**R^2**
3.2801	0.001968	39.67	$-7.68*10^{-3}$	0.99996	-0.02917	-0.02917	0.3150	0.85075

4.7. Adsorption Kinetics

Batch equilibrium experiments were carried out to find the kinetics of adsorption. A 100 ml conical flask was employed at optimum conditions that were 12.8 mg/L of lead (II) ion, pH 5.2, and an adsorbent dosage of 4.5 g zeolite-X, while the equilibrium capacity at the optimum point was 0.343501997 mg/g and the equilibrium concentration of lead (II) ion was 0.0218 mg/L. The time-dependent experimental adsorption data were used for kinetic modeling. To analyze the adsorption kinetics of lead metal ions, the pseudo-first- and pseudo-second-order models were applied to the data in the present study. The square of correlation coefficients, R^2, for the pseudo-first-order model and pseudo-second-order model, were 0.25204 and 0.99956, respectively. The results in Fig. 4.16 and 4.17 show linear plots with very high values of R^2 (Table 4.10). Therefore, the adsorption of Lead (II) ion onto zeolite-X is greatly represented by the pseudo-second-order kinetics. The adsorption of Lead (II) ion onto zeolite-X (Na-X) indicates that the concentration of both zeolite-X and Pb (II) ions were involved in the rate-determining step and the adsorption process was chemisorption.

Table 4.10. Pseudo-first and Pseudo-second order kinetic data for the adsorption of lead ion onto zeolite Na-X

Time	qe	qt	qe-qt	ln(qe-qt)	t/qt
15	0.343501997	0.306180648	0.037321	-3.28819	48.99069
30	0.343501997	0.341369285	0.002133	-6.15036	87.88137
45	0.343501997	0.341684421	0.001818	-6.31025	131.7005
60	0.343501997	0.34346427	3.77E-05	-10.1851	174.6907
75	0.343501997	0.342776298	0.000726	-7.22838	218.8016
90	0.343501997	0.342707501	0.000794	-7.1378	262.6146

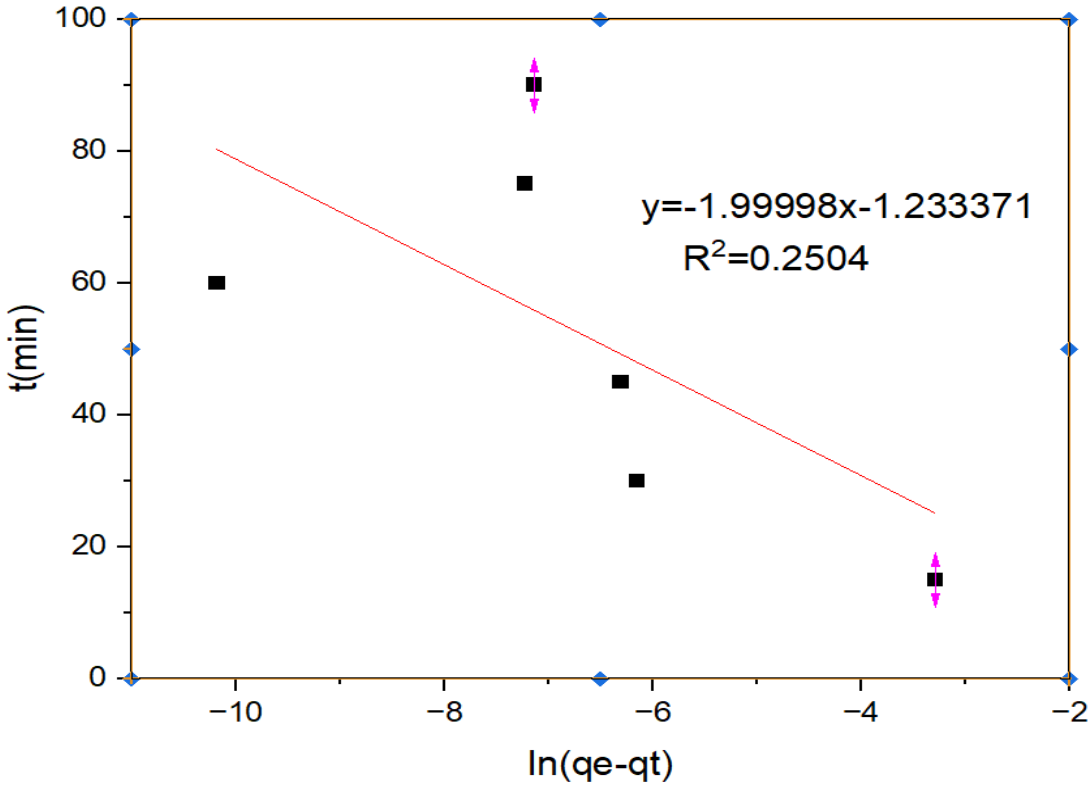

Figure 4.16. Pseudo-first-order kinetic model data plot for the adsorption of lead ion

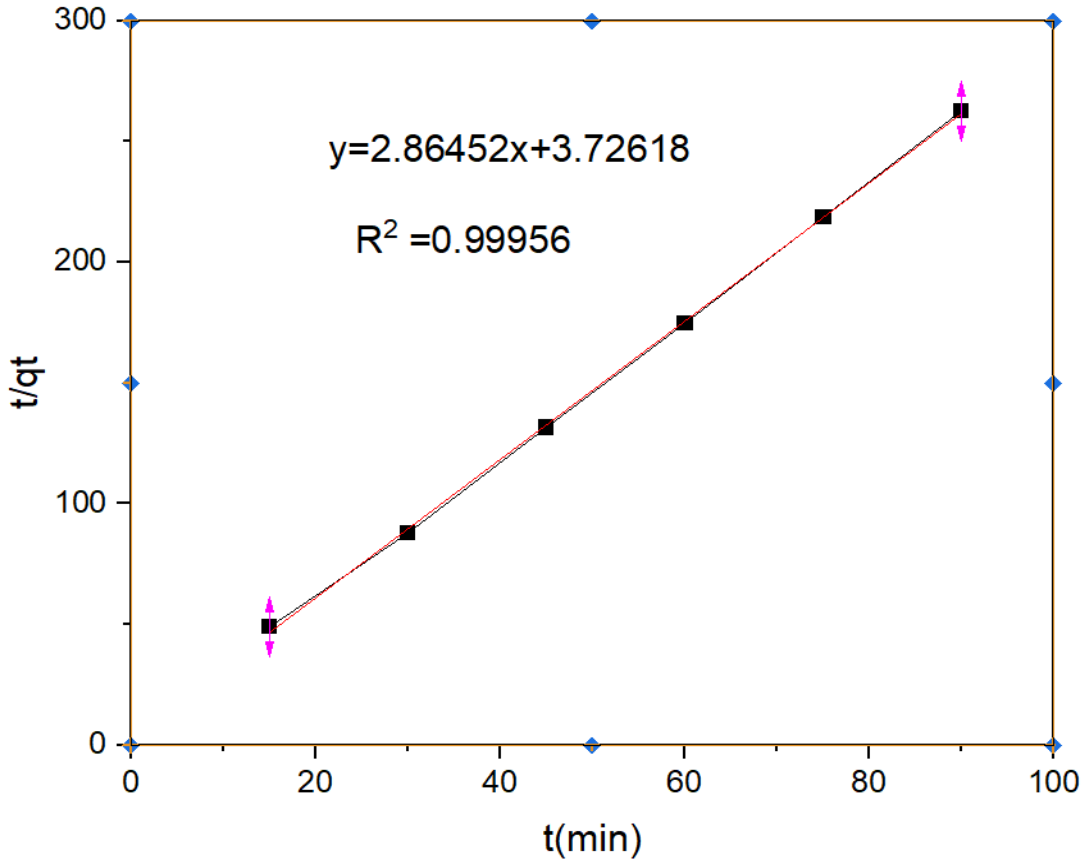

Figure 4.17. Pseudo-second-order kinetic model data plot for the adsorption of lead ion

Table 4.11: Adsorption kinetic parameters of Pb (II) ion zeolite Na-X

	Pseudo first-order kinetic model					**Pseudo- second-order kinetic model**			
intercept	slope	qe(mg/g)	K_1	R^2	Intercept	slope	(qe(mg/g)	K_2	R^2
-1.233371	-1.99998	0.058	-0.0386	0.25204	3.72618	2.86452	0.349099	2.237993209	0.999561

Table 12 showed that Different type of zeolites as adsorbent with the Comparison of sorption capacity of Pb (II) ion concentrations in compass of isotherm model and kinetics model.

Table 4. 12: Lead (II) ion removed by different zeolites, along with experimental conditions and adsorption and kinetic models.

Metal ion	zeolite	T^{o}C	Contact time(h)	Conc.of initial metal ion(mg/L)	pH	Pb(II) sorption mg/g	Isotherm model	Kinetics model
Pb (II)ion	A	25	5	50-800	4	100	Langmuir	Pseudo-second-order
	A	25	0.5	100-400	7.5	182	Langmuir	
	X	25	0.5	100-400	7.5	213		
	Clinoptilolite	70	24	200-2000	4.5	78.7		
	Na-clinoptilolite	70	24	200-2000	4.5	91.2		
	Faujasite Y	25	1	70-400	4.5	25.9	Langmuir	Pseudo-second-order
	Clinoptilolite	206	6	103	8	51.6	Langmuir	
	HDTMA-Y	25	24	1000	0 5	76.0	Langmuir	Pseudo-second-order
	A	25	5	50-800	4 5	6.5	Langmuir	Pseudo-second-order
	NaP1	22	6	10-200	2.56	50.8	Langmuir	
	A	25	25	100-400	7.5	28.6	Langmuir	
	X	25	0.5	100-400	7.5	41.0	Langmuir	
	My work (zeolite-X)	25	51.8min /.97h	12.8	5.2	39.67	Langmuir	Pseudo-second-order

(Irannajad and Kamran Haghighi 2021)

4.8. The Removal Performance of Zeolite on the Real Waste Water

After optimization, analyses were conducted for the synthetic wastewater by Pb (II) ion. Removal efficiency. The analysis was conducted on Nefas silk paint factory waste water under the optimum conditions of Pb (II) removal from synthetic wastewater. Using the optimum conditions for the removal of Pb (II) ions from synthetic wastewater that were constant (T = 25 ^{o}C, rpm = 250, contact time =51.2 min, pH 5.2, adsorbent dose (g) = 4.506) from Nefas silk paint factory wastewater by using zeolite Na-X per 100 ml of wastewater, the removal efficiency of Pb (II) (%) was 90.9%.

The highest concentration of Pb (II) ion in effluent samples obtained from Nifas Silk paint-producing company was 3.014 mg/L in the current study (Table 4.13). The quantity of lead ions identified in paint factory effluent samples did not satisfy the Ethiopian standard (ES), but it also did not meet the limit imposed by the range of the observed concentration of lead compared to the WHO acceptable threshold of 0.01 mg/l.

Table 4. 13:Lead analysis of the treated and untreated paint effluent

Parameter	Untreated waste water	Treated wastewater
Pb (mg/L)	3.014	0.2734
Removal %		90.9 %

Figure 4.20 shows that the zeolite synthesized and the removal efficiency of Pb (II) from real wastewater and synthetic wastewater at the optimum condition. The initial measured concentration of Pb (II) from real wastewater was taken 3.014mg/L. After application of adsorption it was found to be 90.90 % of Pb (II) removal efficiency and adsorption capacity was 6.08 mg/g. This removal result is lower than the removal efficiency of synthetic wastewater in the laboratory, due to the presence of other competitive pollutants in the real wastewater that affect the removal efficiency the zeolite-X.

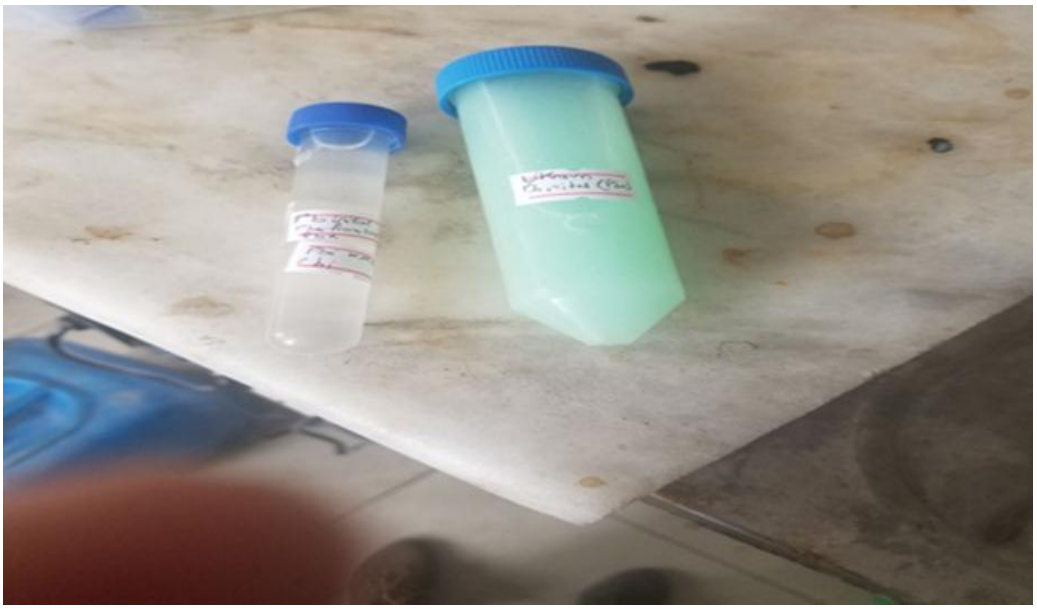

Figure 4. 18: Wastewater before and after adsorption by zeolite-X

Table 4.14. Showed that Different type of zeolites as adsorbent with the Comparison of sorption capacity of Pb (II) ion concentrations.

Table 4. 14: Adsorption performance of lead (II) removal from wastewater by Different Zeolites

Zeolite	T (°C)	Time (h)	Metal conc. (mg/L)	pH	Metal Sorption(mg/g)
Clinoptilolite	70	24	100	4.5	78.7
Clinoptilolite	25	2	10–100	2–7	10
Na-clinoptilolite	70	24	100	4.5	91.2
NaX activated carbon	25	24	1000	7.5	228
Zeolite A	25	0.5	20	7.5	213
Zeolite X	25	0.5	20	7.5	187
My work	25	51.8min/0.97h	12.8	5.2	6.08

(Guida et al. 2020)

5. CONCLUSION AND RECOMMENDATION

5.1. Conclusion

The removal of heavy metals is a vital step in reducing the negative effects caused by their presence in non-target environments. The present work demonstrates that it is possible to prepare synthetic zeolites-X from inexpensive and readily available material kaolin. The formation of zeolite-X framework was revealed by the functionality of the sample as seen by the FTIR and the structure by the XRD diffraction pattern, microstructure (surface morphology) indicated by SEM micrographs as well as surface area indicated by BET.

The optimum conditions of Pb (II) ion removal from synthetic wastewater on the zeolite-X were obtained as pH 5.2, adsorbent dose 4.506 g and initial concentration 12.8mg/L and contact time 51.8minBecause of their structure's surface area and active adsorbent places, the produced Na-zeolites were an excellent material for removing Pb (II) ions from wastewater. The faujasite-based zeolites, on the other hand, were more useful and efficient adsorbents for the removal of Pb (II) ions from wastewater. They may be used to remove heavy metals even at low pollution levels.Based on the result obtained within the framework of this study it appears that the zeolite-X (Na-X) constitutes a good adsorbent for removing pollutants of lead (II) ion from synthetic and paint factory wastewater.In optimum conditions, the removal efficiency of lead from synthetic wastewater and real wastewater was 98.2 and 90.9 % respectively. According to the adsorption isotherm study results, the Langmuir isotherm model gives the best correlation of (R^2), which was determined to be 0.99996. It also suited the adsorption kinetics better than the pseudo-second-order model with the correlation. Finally, this study demonstrated that the zeolite adsorption procedure was a low-cost, environmentally friendly, and effective adsorbent for the treatment of paint industrial wastewater to remove lead (II) ions.

5.2. Recommendation

- ✓ The following recommendations were made for further study in the production and application of zeolite-x and other zeolites for the removal of pollutants from paint factory wastewater.
- ✓ In this study the adsorbent was modified from Kaolin to zeolite–X by using sodium hydroxide in order to increase the negative surface charge of the adsorbent, so further research should be investigated by using different types of acid and base to find even high or 100% removal efficiency.
- ✓ In this study, the zeolite-X from kaolin was conducted with constant impregnation ration, and time to get a good yield of the Zeolite-X, therefore it is recommended further study by using different impregnation ration, and time to find maximum yield.
- ✓ This research was conducted only on the removals of one metal (Pb) from paint wastewater, further work should be conducted on the removal of other heavy metals by using zeolite.
- ✓ The use low cost of synthesized zeolites Na-X in the application of catalysis has been widely highly recommended.
- ✓ As it is known, since the raw material is extracted from the ground, if the government controls the land balance and creates awareness for it to be produced on a large scale and factories use it, it will also contribute to reducing foreign exchange.

References

Afolabi, Felicia O, Musonge, P. and Bakare, B. F. (2021) 'Bio-sorption of copper and lead ions in single and binary systems onto banana peels Bio-sorption of copper and lead ions in single and binary systems onto banana peels', Cogent Engineering, 8(1), pp. 0–14. doi: 10.1080/23311916.2021.1886730.

Afolabi, Felicia O., Musonge, P. and Bakare, B. F. (2021) 'Evaluation of lead (Ii) removal from wastewater using banana peels: Optimization study', Polish Journal of Environmental Studies, 30(2), pp. 1487–1496. doi: 10.15244/pjoes/122449.

Aigbe, R. and Kavaz, D. (2020) 'Chinese Journal of Chemical Engineering Unravel the potential of zinc oxide nanoparticle-carbonized sawdust matrix for removal of lead (II) ions from aqueous solution', Chinese Journal of Chemical Engineering, (xxxx). doi: 10.1016/j.cjche.2020.05.007.

Aigbe, R. and Kavaz, D. (2021) 'Unravel the potential of zinc oxide nanoparticle-carbonized sawdust matrix for removal of lead (II) ions from aqueous solution', Chinese Journal of Chemical Engineering, 29, pp. 92–102. doi: 10.1016/j.cjche.2020.05.007.

Amen, R. et al. (2020) 'Jo ur na l P of', Cleaner Engineering and Technology, p. 100006. doi: 10.1016/j.clet.2020.100006.

Aniyikaiye, T. E. et al. (2019) 'Physico-chemical analysis of wastewater discharge from selected paint industries in Lagos, Nigeria', International Journal of Environmental Research and Public Health, 16(7). doi: 10.3390/ijerph16071235.

Aragaw, T. A. and Ayalew, A. A. (2019) 'Removal of water hardness using zeolite synthesized from Ethiopian kaolin by hydrothermal method', Water Practice and Technology, 14(1), pp. 145–159. doi: 10.2166/wpt.2018.116.

Astuti, W. et al. (2021) 'Chinese Journal of Chemical Engineering Removal of lead (Pb (II)) and zinc (Zn (II)) from aqueous solution using coal fly ash (CFA) as a dual-sites adsorbent', 34, pp. 289–298.

Aziz, A. et al. (2019) ‘Highly porous carboxylated activated carbon from jute stick for removal of Pb 2 + from aqueous solution’, pp. 22656–22669.

B. S. K. Poonam and N. Kumar, Kinetic study of lead (Lead (II) ion) removal from battery manufacturing wastewater using bagasse biochar as biosorbent, Appl. Water Sci., 2018, 8(4), 1–13, DOI: 10.1007/s13201-018-0765-z

Bavel, J. J. V. et al. (2020) ‘Using social and behavioural science to support COVID-19 pandemic response’, Nature Human Behaviour, 4(5), pp. 460–471. doi: 10.1038/s41562-020-0884-z.

Bayuo, J., Abukari, M. A. and Pelig-ba, K. B. (2019) ‘Equilibrium isotherm studies for the sorption of hexavalent chromium (VI) onto groundnut shell’, 11(12), pp. 40–46. doi: 10.9790/5736-1112014046.

Bayuo, J., Rwiza, M. and Mtei, K. (2022a) ‘A comprehensive review on the decontamination of lead(ii) from water and wastewater by low-cost biosorbents’, RSC Advances, 12(18), pp. 11233–11254. doi: 10.1039/d2ra00796g.

Bayuo, J., Rwiza, M. and Mtei, K. (2022b) ‘A comprehensive review on the decontamination of lead(ii) from water and wastewater by low-cost biosorbents’, RSC Advances, 12(18), pp. 11233–11254. doi: 10.1039/d2ra00796g.

Boontham, W. (2016) ‘Removal of lead from solution by using low cost adsorbents from aplaceae family’.

Bouabidi, Z. B. et al. (2017) ‘Steel-Making dust as a potential adsorbent for the removal of lead (II) from an aqueous solution’, Chemical Engineering Journal, (Ii). doi: 10.1016/j.cej.2017.10.073.

Bright Kwakye-Awuah, Elizabeth Von-Kiti, Isaac Nkrumah, Rose Erdoo

Chai, J. B. et al. (2020) ‘Adsorption of heavy metal from industrial wastewater onto low-cost Malaysian kaolin clay–based adsorbent’, Environmental Science and Pollution Research, 27(12), pp. 13949–13962. doi: 10.1007/s11356-020-07755-y.

Chowdhury, I. R. et al. (2022) Removal of lead ions (Lead (II) ion) from water and wastewater: a review on the low-cost adsorbents, Applied Water Science. Springer International Publishing. doi: 10.1007/s13201-022-01703-6.

Cooper, D., Doucet, L. and Pratt, M. (2007) 'Understanding in multinational organizations', Journal of Organizational Behavior, 28(3), pp. 303–325. doi: 10.1002/j.

Cordova Estrada, A. K., Cordova Lozano, F. and Lara Díaz, R. A. (2021) 'Thermodynamics and Kinetic Studies for the Adsorption Process of Methyl Orange by Magnetic Activated Carbons', Air, Soil and Water Research, 14. doi: 10.1177/11786221211013336.

Editorial, E. et al. (2020) 'Zeolites'.

Endale, Y. T. et al. (2021) 'Exposure and health risk assessment from consumption of Pb contaminated water in Addis Ababa, Ethiopia', Heliyon, 7(9), p. e07946. doi: 10.1016/j.heliyon.2021.e07946.

Fanta, F. T. et al. (2019) 'Copper doped zeolite composite for antimicrobial activity and heavy metal removal from waste water', BMC Chemistry, 13(3). doi: 10.1186/s13065-019-0563-1.

Fu, F. and Wang, Q. (2011) 'Removal of heavy metal ions from wastewaters: A review', Journal of Environmental Management, pp. 407–418. doi: 10.1016/j.jenvman.2010.11.011.

Gebregziabher, B., Kassahun, S. K. and Kiflie, Z. (2021) 'Statistical optimization of mixed peanut shell and Khat (Catha edulis) stem carbonization process for molasses enhanced cold and low-pressure pelletization', Biomass Conversion and Biorefinery. doi: 10.1007/s13399-021-01446-5.

Gougazeh, M., Buhl, J. and Gougazeh, M. (2018) 'Journal of the Association of Arab Universities for Basic Synthesis and characterization of zeolite A by hydrothermal transformation of natural Jordanian kaolin Synthesis and characterization of zeolite A by hydrothermal transformation of natural Jordania', Journal of the Association of Arab Universities for Basic and Applied Sciences, 15, pp. 35–42. doi: 10.1016/j.jaubas.2013.03.007.

Grela, A. et al. (2018) 'Characterization of the products obtained from alkaline conversion of tuff and metakaolin', Journal of Thermal Analysis and Calorimetry, 133(1), pp. 217–226. doi: 10.1007/s10973-018-6970-z.

Hamere Yohannes and Eyasu Elias (2017) 'Contamination of Rivers and Water Reservoirs in and Around Addis Ababa City and Actions to Combat It', Environment Pollution and Climate Change, 1(2), pp. 1–12.

Hussain, T. et al. (2021) 'Synthesis and Characterization of Na-Zeolites from Textile Waste Ash and Its Application for Removal of Lead (Pb) from Wastewater'.

Hussain, T.; Hussain, A.I.; Chatha, S.A.S.; Ali, A.; Rizwan, W.; Ali, S.; Ahamd, P.; Wijaya, L.; Alyemeni, M.N (2021), Synthesis and Characterization of Na-Zeolites from Textile Waste Ash and Its Application for Removal of Lead (Pb) from Wastewater. Int. J. Environ. Res. Public Health, 18, 3373. https://doi.org/ 10.3390/ijerph18073373

Ikyreve, Iza Radecka & C. Williams (2016): Parametric, equilibrium, and kinetic study of the removal of salt ions from Ghanaian seawater by adsorption onto zeolite X, Desalination and Water Treatment, DOI: 10.1080/19443994.2015.1128361

Irfan Khan, M. et al. (2017) 'The pyrolysis kinetics of the conversion of Malaysian kaolin to metakaolin', Applied Clay Science, 146(May), pp. 152–161. doi: 10.1016/j.clay.2017.05.017.

J. Bayuo, K. B. Pelig-ba, M. Abdullaiabukari and M. A. Abukari, Isotherm Modeling Of Lead(II) Adsorption From Aqueous Solution Using Groundnut Shell As A LowCost Adsorbent, IOSR J. Appl. Chem., 2018, 11(11), 18–23.

J. Bayuo, M. A. Abukari and K. B. Pelig-ba, Equilibrium isotherm studies for the sorption of hexavalent chromium(VI) onto groundnut shell, IOSR J. Appl. Chem., 2019, 11(12), 40–46.

Jos, F. et al. (2018) 'Removal of Pb 2 + in Wastewater via Adsorption onto an Activated Carbon Produced from Winemaking Waste'. doi: 10.3390/met8090697.

Joseph, L. et al. (2019) ‘Chemosphere Removal of heavy metals from water sources in the developing world using low-cost materials : A review’, Chemosphere, 229, pp. 142–159. doi: 10.1016/j.chemosphere.2019.04.198.

Joseph, L.; Jun, B.-M.; Flora, J.R.; Park, C.M.; Yoon, Y. Removal of heavy metals from water sources in the developing world using low-cost materials: A review. Chemosphere 2019, 229, 142–159.

Kabwadza-corner, P., Johan, E. and Matsue, N. (2015) ‘pH Dependence of Lead Adsorption on Zeolites’, (January). doi: 10.4236/jep.2015.61006.

Kassahun, S. K. et al. (2017) ‘Optimization of sol-gel synthesis parameters in the preparation of N-doped TiO2 using surface response methodology’, Journal of Sol-Gel Science and Technology, 82(2), pp. 322–334. doi: 10.1007/s10971-017-4322-2.

Khandanlou, R. et al. (2015) ‘Rapid Adsorption of Copper (II) and Lead (II) by Rice Straw / Fe 3 O 4 Nanocomposite : Optimization, Equilibrium Isotherms, and Adsorption Kinetics Study’, (Ii), pp. 1–19. doi: 10.1371/journal.pone.0120264.

Kwakye, R. et al. (2022) ‘Characterization of Metakaolin from Wassa Kaolin and Its Potential as Adsorbent for the Regeneration of Used Engine Lubrication Oil’, Advances in Materials Science and Engineering, 2022. doi: 10.1155/2022/4805410.

Kwakye-Awuah, B. et al. (2016) ‘Parametric, equilibrium, and kinetic study of the removal of salt ions from Ghanaian seawater by adsorption onto zeolite X’, Desalination and Water Treatment, 57(45), pp. 21654–21663. doi: 10.1080/19443994.2015.1128361.

M.Irfan Khan, Hafeez Ullah Khan, Khairun Azizli, Suriati Sufian, Zakaria Man, Ahmer AliSiyal, Nawshad Muhammad,M.Faiz ur Rehman, (2017), The pyrolysis kinetics of the conversion of Malaysian kaolin to metakaolin, Applied Clay Science, 146, , 152-161.

Mabuza, M., Premlall, K. and Daramola, M. O. (2022) ‘Modelling and thermodynamic properties of pure CO2 and flue gas sorption data on South African coals using Langmuir, Freundlich, Temkin, and extended Langmuir isotherm models’, International Journal of Coal Science and Technology, 9(1). doi: 10.1007/s40789-022-00515-y.

Markovska, I. (2018) ‘Synthetic Zeolites - Structure, Clasification, Current Trends In Zeolite Synthesis - D_Georgiev.pdf’, And International Science Conference: Economics and Society Develop, (September 2009), pp. 1–6. Available at: http://www.sustz.com/Proceeding09/Papers/Technical studies/D_GEORGIEV.pdf.

Masoudian, S. K., Sadighi, S. and Abbasi, A. (2013) ‘Synthesis and characterization of high aluminum zeolite X from technical grade materials’, Bulletin of Chemical Reaction Engineering and Catalysis, 8(1), pp. 54–60. doi: 10.9767/bcrec.8.1.4321.54-60.

Medina-Rodríguez, D. F. et al. (2021) ‘Removal of pb(II) in aqueous solutions using synthesized zeolite x from ecuadorian clay’, Ingenieria e Investigacion, 41(2). doi: 10.15446/ing.investig.v41n2.89671.

Mekuria, D. M., Kassegne, A. B. and Asfaw, S. L. (2020) ‘Little Akaki River sediment enrichment with heavy metals , pollution load and potential ecological risks in downstream , Central Ethiopia’, Environmental Systems Research. doi: 10.1186/s40068-020-00188-z.

Menbere, M. P. (2019) ‘Industrial Wastes and Their Management Challenges in Ethiopia’, pp. 1–6.

Moshoeshoe, M., Silas Nadiye-Tabbiruka, M. and Obuseng, V. (2017) ‘A Review of the Chemistry, Structure, Properties and Applications of Zeolites’, American Journal of Materials Science, 2017(5), pp. 196–221. doi: 10.5923/j.materials.20170705.12.

Mustapha, S. et al. (2019) ‘Adsorption isotherm, kinetic and thermodynamic studies for the removal of Pb(II), Cd(II), Zn(II) and Cu(II) ions from aqueous solutions using Albizia lebbeck pods’, Applied Water Science, 9(6), pp. 1–11. doi: 10.1007/s13201-019-1021-x.

Narayanan, S. L. and Vetha, G. V. I. (2017) ‘Equilibrium studies on removal of lead (II) ions from aqueous solution by adsorption using modified red mud’, International Journal of Environmental Science and Technology, (Ii). doi: 10.1007/s13762-017-1513-x.

Nguyen, T. C., Loganathan, P. and Nguyen, T. V. (2017) ‘Adsorptive removal of five heavy metals from water using blast furnace slag and fly ash’. doi: 10.1007/s11356-017-9610-4.

Nur-E-Alam, M. et al. (2020) ‘An overview of chromium removal techniques from tannery effluent’, Applied Water Science, 10(9), pp. 1–22. doi: 10.1007/s13201-020-01286-0.

Odaracha, S. L. et al. (2021) ‘Multivariate Optimization of Pb 2+ Adsorption onto Ethiopian Low-Cost Odaracha Soil Using Response Surface Methodology’.

Olaremu, A. G. et al. (2018) ‘Synthesis of zeolite from kaolin clay from Erusu Akoko southwestern Nigeria’, J. Chem Soc. Nigeria, 43(3), pp. 381–786. Available at: https://journals.chemsociety.org.ng/index.php/jcsn/article/view/188.

Panek, R. et al. (2021) ‘Simultaneous Removal of Pb 2 + and Zn 2 + Heavy Metals Using Fly Ash Na-X Zeolite and its Carbon Na-X (C) Composite’, (C), pp. 1–18.

Pfeifer, A., Škerget, M. and Čolnik, M. (2020) ‘Removal of iron , copper , and lead from aqueous solutions with zeolite , bentonite , and steel slag .’, Separation Science and Technology, 00(00), pp. 1–12. doi: 10.1080/01496395.2020.1866607.

Rahman, I. et al. (2022) Removal of lead ions - (Pb 2 +) from water and wastewater : a review on the low ‐ cost adsorbents, Applied Water Science. Springer International Publishing. doi: 10.1007/s13201-022-01703-6.

Safatian, F. et al. (2019) ‘Lead ion removal from water by hydroxyapatite nanostructures synthesized from egg sells with microwave irradiation’, Applied Water ScienceFatemeh, 9(4), pp. 1–6. doi: 10.1007/s13201-019-0979-8.

Shrestha, A. M., Neupane, S. and Bisht, G. (2017) ‘An Assessment of Physicochemical Parameters of Selected Industrial Effluents in Nepal’, 2017.

Sime, T. (2018) ‘Investigation of Activated Carbon as Adsorbent For Paint Industry Wastewater Treatment Addis Ababa Science and Technology University’.

State, R. et al. (2020) ‘Synthesis of Zeolite X from Locally Sourced Kaolin Clay from Kono-Boue and Chokocho ’, pp. 399–407. doi: 10.4236/aces.2020.104025.

Tadesse, M., Tsegaye, D. and Girma, G. (2018) ‘Assessment of the level of some physico-chemical parameters and heavy metals of Rebu river in oromia region, Ethiopia’, 2(3). doi: 10.15406/mojbm.2018.03.00085.

Tesfaye, D. (2016) 'School of Chemical and Bio Engineering Removal of Lead From Waste Water Using Corn Cob Activated Carbon As an Adsorbent'.

Tessema, T. S., Adugna, A. T. and Kamaraj, M. (2020) 'Removal of Pb (II) from Synthetic Solution and Paint Industry Wastewater Using Activated Carbon Derived from African Arrowroot (Canna indica) Stem', Advances in Materials Science and Engineering, 2020. doi: 10.1155/2020/8857451.

Tsvetanova, L. et al. (2022) 'Equilibrium Isotherms and Kinetic Effects during the Adsorption of Pb (II) on Titanosilicates Compared with Natural Zeolite Clinoptilolite', Water (Switzerland), 14(14). Doi: 10.3390/w14142152.

Udeh, N.U, Agunwamba, J. . (2017) 'Equilibrium and Kinetics Adsorption of Cadmium and Lead Ions from Aqueous Solution Using Bamboo Based Activated Carbon', pp. 17–26.

Udeh, N.U1, Agunwamba, J.C, Equilibrium and Kinetics Adsorption of Cadmium and Lead Ions from Aqueous Solution Using Bamboo Based Activated Carbon The International Journal Of Engineering And Science (IJES) 6, 2, 17-26 , 2017. DOI : 10.9790/1813-0602011726 www.theijes.com.

Wambu, E. W. et al. (2018) 'Removal of heavy-metals from wastewater using a hydrous alumino-silicate mineral from Kenya', Bulletin of the Chemical Society of Ethiopia, 32(1), pp. 39–51. doi: 10.4314/bcse.v32i1.4.

Waste, W. et al. (2021) 'High Efficiency of the Removal Process of Pb (II) and Cu (II) Ions with the Use of Fly Ash from Incineration of Sunflower and', (Ii).

Woldeamanuale, T. B. (2017) 'Toxicity Study of Heavy Metals Pollutants and Physico-Chemical Characterization of Effluents Collected from Different Paint Industries in Addis Ababa, Ethiopia', Journal of Forensic Sciences & Criminal Investigation, 6(2), pp. 1–6. doi: 10.19080/jfsci.2017.06.555685.

Yang, X.; Xia, L.; Song, S. Arsenic adsorption from water using graphene-based materials as adsorbents: A critical review. Surf. Rev. Lett. 2017, 24, 1730001

Zewdie, T. M. et al. (2021) 'Characterization and Beneeciation of Ethiopian Kaolin for use in Fabrication of Ceramic Membrane Abhishek Dutta Izmir Institute of Technology Gulbahce Campus: Izmir Yuksek Teknoloji Enstitusu Characterization and beneficiation of Ethiopian kaolin for use '. doi: 10.21203/rs.3.rs-646050/v1.

Appendices

Appendix 1.1 Build Information

File Version	13.0.1.0		
Study Type	Response Surface	**Subtype**	Randomized
Design Type	Box-Behnken	**Runs**	29.00
Design Model	Quadratic	**Blocks**	No Blocks
Build Time (ms)	1.0000		

Appendix. 1.2 factors

Factor	Name	Units	Type	SubType	Minimum	Maximum	Coded Low	Coded High	Mean	Std. Dev.
A	CONTACT TIME	MIN	Numeric	Continuous	15.00	90.00	-1 ↔ 15.00	+1 ↔ 90.00	52.50	24.55
B	CONC. of adsorbant	g	Numeric	Continuous	0.5000	5.00	-1 ↔ 0.50	+1 ↔ 5.00	2.75	1.47
C	CONC,OF Pb	mg/L	Numeric	Continuous	1.0000	30.00	-1 ↔ 1.00	+1 ↔ 30.00	15.50	9.49
D	pH		Numeric	Continuous	3.00	9.00	-1 ↔ 3.00	+1 ↔ 9.00	6.00	1.96

Appendix 1.3. Responses

Response	Name	Units	Observations	Minimum	Maximum	Mean	Std.Dev.	Ratio
R1	removal of Pb efficiency	%	29.00	85.3	98.2	94.44	4.34	1.15

Appendix 1.4. Fit Summary, Response 1: removal of Pb efficiency

Source	Sequential p-value	Lack of Fit p-value	Adjusted R^2	Predicted R^2	
Linear	< 0.0001	0.0005	0.6020	0.5158	
2FI	0.9894	0.0003	0.4926	0.1458	
Quadratic	**< 0.0001**	**0.1689**	**0.9828**	**0.9549**	**Suggested**
Cubic	0.0436	0.7519	0.9942	0.9743	**Aliased**

Appendix 1.5. Sequential Model Sum of Squares [Type I]

Source	Sum of Squares	df	Mean Square	F-value	p-value	
Mean vs Total	2.586E+05	1	2.586E+05			
Linear vs Mean	346.76	4	86.69	11.59	< 0.0001	
2FI vs Linear	7.86	6	1.31	0.1373	0.9894	
Quadratic vs 2FI	**167.14**	**4**	**41.79**	**129.05**	**< 0.0001**	**Suggested**
Cubic vs Quadratic	3.87	8	0.4842	4.41	0.0436	Aliased
Residual	0.6591	6	0.1098			
Total	2.592E+05	29	8936.81			

Select the highest order polynomial where the additional terms are significant and the model is not aliased.

Appendix 1.6. Model Summary Statistics

Source	Std. Dev.	R^2	Adjusted R^2	Predicted R^2	PRESS	
Linear	2.74	0.6589	0.6020	0.5158	254.85	
2FI	3.09	0.6738	0.4926	0.1458	449.56	
Quadratic	**0.5690**	**0.9914**	**0.9828**	**0.9549**	**23.71**	**Suggested**
Cubic	0.3314	0.9987	0.9942	0.9743	13.50	Aliased

Focus on the model maximizing the Adjusted R^2 and the Predicted R^2.

Appendix 1.7 Lack of Fit Tests

Source	Sum of Squares	df	Mean Square	F-value	p-value	
Linear	178.96	20	8.95	62.63	0.0005	
2FI	171.10	14	12.22	85.54	0.0003	
Quadratic	**3.96**	**10**	**0.3962**	**2.77**	**0.1689**	**Suggested**
Cubic	0.0876	2	0.0438	0.3065	0.7519	Aliased
Pure Error	0.5715	4	0.1429			

Laboratory pictures

Kaolin

washed kaolin

Mixed dried kaolin and mixed NaOH


Fusion of alkaline used by ballast furnace grinded


Powder of meta-kaolin


Agitated material at 100^{O}c and at room temperature for 24h

Filtated formed the zeoilte-x

Dried Zeolite-X formed and powder form of zeolite -x


Batched adsorption experiment

After batch of adsorption experiment